universe MDPI

Review

Revisiting Hansen's Ideal Frame Propagation with Special Perturbations—1: Basic Algorithms for Osculating Elements

Martin Lara [1,*] and **Hodei Urrutxua** [2]

[1] Scientific Computation & Technical Innovation Center, Universidad de La Rioja, C. Madre de Dios, 53, 26006 Logroño, La Rioja, Spain
[2] Fuenlabrada Engineering School, Universidad Rey Juan Carlos, Camino del Molino, 5, 28943 Fuenlabrada, Madrid, Spain; hodei.urrutxua@urjc.es
* Correspondence: mlara0@gmail.com

Abstract: A review of the basic Hansen's ideal frame algorithms for accurate numerical integration of perturbed elliptic motion is carried out. The fundamental approaches rely on the use of nonsingular variables and differ in the ways in which the ellipse in the orbital plane is determined. It is well known that the accuracy of the propagation of the orbit geometry is notably increased when using time-regularization techniques to transform the independent variable. However, this is at the expense of adding a differential equation to compute the time, which gathers the Lyapunov-type instabilities that are removed from the coordinates. The asynchronism resulting from errors in the numerical integration of the time may be palliated with the use of time elements, to which end a constant and a linear nonsingular time element are presented, which are new to our knowledge.

Keywords: orbit propagation; perturbed Kepler motion; variation of parameters; ideal frames; ideal elements; time regularization; time elements; special perturbations; Hamilton–Jacobi equation; extended phase space

check for updates

Citation: Lara, M.; Urrutxua, H. Revisiting Hansen's Ideal Frame Propagation with Special Perturbations—1: Basic Algorithms for Osculating Elements. *Universe* **2023**, *9*, 470. https://doi.org/10.3390/universe9110470

Academic Editor: Lorenzo Iorio

Received: 25 September 2023
Revised: 28 October 2023
Accepted: 29 October 2023
Published: 31 October 2023

1. Introduction

Special perturbation methods in orbital mechanics follow two basic approaches. On the one hand, the use of coordinates as the integration variables notably eases the implementation of the differential equations for typical celestial mechanics and astrodynamics problems and provides the solution in a form useful for ephemeris prediction. The classical Encke and Cowell methods are usually programmed in Cartesian coordinates [1–4], but more sophisticated approaches such as those based on KS or projective coordinates are customary, too [5–8]. On the other hand, the use of "elements" (or "parameters") as the integration variables for perturbation problems—whose variations remain constant in the simplifications of the unperturbed, integrable model and which are commonly obtained as different combinations of its basic integrals—allows for more stable propagation of the initial state. However, this is at the cost of more involved programming, which may need the inclusion of a variety of routines to transform the elements into coordinates in order to obtain the ephemeris, when required.

For perturbed Keplerian motion, classical implementations of the variation-of-parameters method rely on the use of elliptic orbital elements or related nonsingular variables [9–13], yet alternative vectorial implementations may enjoy more symmetric formulations due to the fact that they gather the differential equations of the slowly varying elements into two vectorial equations, which, therefore, are simpler to code and faster to evaluate [14–22]. Because of that, the latter fit very well for automatic computing and hence have become very popular nowadays, especially regarding the long-term propagation of average dynamics [23–29]. In either case, the characteristics of elliptic motion require an uneven step-size distribution for optimal numerical integration, with shorter steps near periapsis and larger ones near apoapsis. While numerical step-size regulation is the aim of different numerical solvers [30–33], analytical step-size regulation by means of time-regularization strategies [6–8,34–42] allows for the use of simpler, robust, and highly efficient fixed-step integration methods. Moreover, it provides definite stabilization of the numerical integration procedure by constraining the effects of the Lyapunov-type instability—which is unavoidably attached to Keplerian dynamics—to the integration of the physical time, which now plays the role of one more dependent variable of the differential system [43–45].

In a mixed way, Cowell-type implementations of the perturbed Keplerian dynamics may have clear benefits from concomitant integration in Cartesian coordinates of one or more of the invariants of the Kepler problem. While the implementation of the differential equations remains analogously simple in this case, projection methods can be used to preserve the geometric properties of the perturbed motion with a minor increase in the computational burden [46,47]. Still, the integration of elements alone is generally regarded as more stable and efficient than any variant of the Cowell- or Encke-type integrations [21,48,49]. Indeed, the propagation of slowly varying elements would allow for much longer step sizes for the numerical solver than in the case of much faster evolving coordinates, in this way largely compensating for the more involved evaluation of the variations in the elements in each computation step. Note, however, that this fact does not deny the utility of coordinates for numerical integration, which show remarkable performance in the case of KS or projective methods [50–52]. Moreover, beyond the perturbed Keplerian dynamics, as may be the case for N-body regimes, coordinate-based methods usually provide higher stability characteristics and are customarily used.

Among the different sets of variations of parameter methods, those based on Hansen's ideal frame [53], for which rotation under perturbations occurs along the instantaneous radius vector, enjoy unique merits for such orbital configurations in which the role played by the orbital plane is significant enough [22,54,55]. In these cases, the orbital motion can be viewed as the composition of two different effects. Namely, the slow rotation of the orbital plane and the fast rotation of the particle within the orbital plane. In spite of fast and slow effects not being decoupled, the fact that the velocity is the same when measured by Hansen's ideal frame as when calculated by the inertial frame presents this approach as an appealing formulation. Indeed, compared to orbital or nodal frame formulations, the ideal frame brings the motion very close to the separation by removing the first derivatives of the variables related to the attitude of the orbital plane from the equations related to the motion in the orbital plane [56]. It must be noted, however, that in those cases for which the role of the orbital plane is not relevant, as happens when the perturbations in the out-of-plane direction are large, or in the case of rectilinear or almost-rectilinear orbits, other approaches may certainly be more effective [21,57,58].

The quest for higher efficiency in the numerical integration of perturbed Keplerian motion over the years has led to recurrent refinements of Hansen's ideal frame formulations that can be efficiently implemented as operational software [59,60]. Basically, extant formulations are limited to two different, quite effective approaches. The *hodographic* approach pinpoints the elements describing the evolution of the eccentricity vector of the osculating orbit, or, more precisely, the coordinates of the center of the velocity hodograph, whereas the *orbital* approach relies on the use of projective coordinates to linearize the radial motion. While these methods clearly differ from each other on how to materialize the polar coordinates in the orbital plane, the two avoid singularities in the description of the attitude of the orbital plane by using Euler parameters and the Rodrigues rotation formula [61]. In both cases, too, the variation of the polar angle defines a finite rotation from the ideal to the orbital frame, whereas the total angular momentum is integrated from the corresponding variation equation.

Rather than using the physical time as the independent variable, popular versions of these two approaches [62–66] find an accurate description of the orbit geometry, as well as efficient numerical integration, by referring the integration to a fictitious time based on a Sundman-type transformation that involves some power of the orbit radius [67,68].

More precisely, the time transformation is commonly stated by a differential equation relating the variations to the physical and fictitious times by a coefficient that involves some power of the radius and a regularizing term. The case in which the exponent of the former is one plays a fundamental role in the integration of the three-body problem [67,69,70], whereas the choice of two for the exponent has been common in planetary theories after Laplace [71,72]. Additionally, raising the radius to three halves shows important advantages regarding the control of truncation errors in numerical integration [36,73]. This latter case was first examined in relation to space exploration [74,75], yet it also finds application in classical celestial mechanics problems [76]. Regarding the regularizing term, it may depend generally on any orbital variable as well as on the total energy [6,77–79]. This is the noteworthy case of time regularizations originally proposed in [80] (see also [39]), a variant of which has been tested in the framework of the ideal frame integration with encouraging results [65].

Alternatively, the need for redundant variables stemming from the use of Euler parameters is kept to a minimum without losing any merit of the ideal-element formulation when re-scaling the Euler parameters by the total angular momentum [81,82]. While the integration of the modulus of the angular momentum is now dispensable, this is at the cost of a slightly more complicated form of the variations of the attitude-related variables. Preliminary computations demonstrated that this simpler formulation may be, in addition, more effective in terms of computing time. However, this conclusion cannot be taken as definitive as far as it is based on the use of a single numerical solver, whereas it is well known that the performance of numerical integration of a particular problem may vary depending on the numerical solver used for propagation [83].

On the other hand, it is known that the accuracy of the solution of time-regularized differential equations may be increased when replacing the numerical integration of the physical time by the alternative integration of time elements [43,77,84–86]. The efficient time element proposed in [80] deserves special mention in reference to analytical perturbations based on (true anomaly) Delaunay-similar variables [87,88], but that also applies to nonsingular variables [89]. Adoption of this linear element four decades later as a time element of the ideal-frame setting showed exceptional accuracy in the numerical integration of circumterrestrial orbits [90]. The improvements to the determination of the physical time introduced with the use of a variety of existing time elements are expected to affect the different formulations presented equally. While we do not discuss this topic yet due to the lack of accessible, detailed descriptions in the literature, we provide in Appendix A the solution to the Hamilton–Jacobi equation of the Kepler problem in the extended phase space, which gives rise to a remarkable set of variables that include the time element and the total energy of the perturbation problem among them. We believe that the exercise is worth being carried out because not only does the popular, linear time element of the (true anomaly) Delaunay-similar variables emerge in the procedure [80,91], but this kind of solution relies on a set of auxiliary, non-osculating functions that are repeatedly reported in the literature [39] and, in particular, are related to the ideal-frame formulation [65,90]—whose merits when used in a special perturbation approach are discussed elsewhere. Moreover, as was expected from the Hamilton–Jacobi solution of the standard Kepler problem [92–94], the solution in the extended phase space is also expedited when using polar canonical coordinates instead of the usual approach in spherical coordinates [77,80,87].

The outline of the paper is as follows. In Section 2, we recall the basics of the Kepler problem, the orbital and hodographic solutions to which provide the common variables and elements used in the integration of perturbed Keplerian motion. Next, the relevant, nonsingular equations of the ideal frame formulation are presented in Section 3, where we also discuss the pros and cons of replacing the integration of the fast-evolving, in-track variable by the integration of an element. The time regularization of the ideal-element variations is considered in Section 4, where the suitability of the radial variables for integration in the fictitious-time scale is shown. The convenience of using time elements instead of integrating the physical-time variation is further elaborated in this section, too.

This is followed by the presentation in Section 5 of alternative formulations based on the ideal frame concept. However, the variety of refinements and applications of Hansen's theory that exist without constraint for the case of elliptic motion are not discussed in this review, and interested readers are referred to [42] for additional information.

2. The Orbital Plane and the Geometry of the Kepler Problem

In an inertial, space frame $(O, \boldsymbol{i}, \boldsymbol{j}, \boldsymbol{k})$, we denote $\boldsymbol{x}$ the position vector of a mass point with respect to the origin and denote

$$\boldsymbol{X} = \frac{\mathrm{d}\boldsymbol{x}}{\mathrm{d}t}, \tag{1}$$

its velocity, with t denoting the physical time. Define the angular momentum vector (per unit mass) as

$$\boldsymbol{G} = \boldsymbol{x} \times \boldsymbol{X} = \Theta \boldsymbol{n}, \tag{2}$$

where $\Theta = \|\boldsymbol{G}\|$ and $\boldsymbol{n} = \boldsymbol{G}/\Theta$. Define also the eccentricity vector

$$\boldsymbol{e} = \frac{1}{\mu}\boldsymbol{X} \times \boldsymbol{G} - \boldsymbol{u}, \tag{3}$$

where $\boldsymbol{u} = \boldsymbol{x}/r$ and $r = \|\boldsymbol{x}\|$. Note the orthogonality constraint $\boldsymbol{G} \cdot \boldsymbol{e} = 0$.

2.1. The Orbital Plane

The unit vector $\boldsymbol{n}$ defines the instantaneous orbital plane. Based on it, we define the moving *orbital frame* $(O, \boldsymbol{u}, \boldsymbol{v}, \boldsymbol{n})$, where $\boldsymbol{v} = \boldsymbol{n} \times \boldsymbol{u}$. Let us also consider a reference frame $(O, \boldsymbol{u}^*, \boldsymbol{v}^*, \boldsymbol{n})$ and denote θ the polar angle in the orbital plane reckoning the position of the orbital frame with respect to the reference frame. That is,

$$\boldsymbol{u} = \boldsymbol{u}^* \cos\theta + \boldsymbol{v}^* \sin\theta, \tag{4}$$

$$\boldsymbol{v} = \boldsymbol{v}^* \cos\theta - \boldsymbol{u}^* \sin\theta. \tag{5}$$

As customary after Cayley, we denote the instantaneous direction $\boldsymbol{u}^*$ as a *departure point* in the orbital frame [95,96].

From the theorem of the moving frame (Coriolis theorem)

$$\boldsymbol{X} = \left(\frac{\mathrm{d}\boldsymbol{x}}{\mathrm{d}t}\right)_{\omega} + \boldsymbol{\omega} \times \boldsymbol{x}, \tag{6}$$

where the time derivative is computed in the moving frame, which rotates with angular velocity $\boldsymbol{\omega} = (\mathrm{d}\theta/\mathrm{d}t)\boldsymbol{n}$. Then, replacing $\boldsymbol{x} = r\boldsymbol{u}$ in Equation (6) and taking into account that $\boldsymbol{u}$ remains constant in the rotating frame, we obtain

$$\boldsymbol{X} = \frac{\mathrm{d}r}{\mathrm{d}t}\boldsymbol{u} + r\boldsymbol{\omega} \times u = \frac{\mathrm{d}r}{\mathrm{d}t}\boldsymbol{u} + r\frac{\mathrm{d}\theta}{\mathrm{d}t}\boldsymbol{v}, \tag{7}$$

which turns Equation (2) into

$$\boldsymbol{G} = r^2\frac{\mathrm{d}\theta}{\mathrm{d}t}\boldsymbol{n}, \tag{8}$$

and yields the fundamental relation

$$\frac{\mathrm{d}\theta}{\mathrm{d}t} = \frac{\Theta}{r^2}. \tag{9}$$

Moreover, again using the theorem of the moving frame and in view of Equation (9), we obtain

$$\frac{\mathrm{d}\boldsymbol{u}}{\mathrm{d}t} = \boldsymbol{\omega} \times u = \frac{\Theta}{r^2}\boldsymbol{v}. \tag{10}$$

Then, replacing Equations (9) and (10) in Equation (7) and denoting the radial velocity $R \equiv \mathrm{d}r/\mathrm{d}t$, we obtain the decomposition

$$\boldsymbol{X} = R\boldsymbol{u} + \frac{\Theta}{r}\boldsymbol{v}. \tag{11}$$

For illustration purposes of the orbit geometry and the different frames used in what follows, the reader is referred to Figure 1.

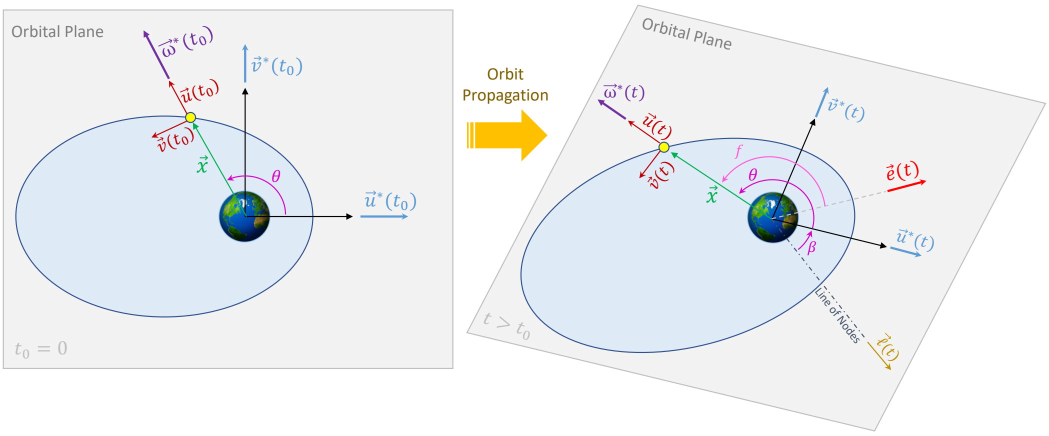

Figure 1. Orbital and ideal frames. For clarity of the figure, the arbitrary choice for the reference frame $(\boldsymbol{u}^*, \boldsymbol{v}^*)$ was done in coincidence with the apsidal frame at t_0. See the text for the used notation.

2.2. The Keplerian Hodograph

In general, all the introduced vectors vary with time under the action of forces according to the laws of mass point dynamics. In the particular case of Newtonian dynamics and the Kepler problem,

$$\frac{\mathrm{d}\boldsymbol{X}}{\mathrm{d}t} = -\frac{\mu}{r^2}\boldsymbol{u}, \tag{12}$$

where μ denotes the gravitational parameter. Then, from differentiation of Equations (2) and (3), it is simple to check that the vectors $\boldsymbol{G}$ and $\boldsymbol{e}$ become constant, in this way comprising the needed integrals that make the Kepler problem solvable.

Using Equation (9), we rewrite Equation (12) as

$$\frac{\mathrm{d}\boldsymbol{X}}{\mathrm{d}\theta} = -\frac{\mu}{\Theta}\boldsymbol{u}, \tag{13}$$

which, in view of Equations (4) and (5), is trivially integrated to yield the trajectory

$$\boldsymbol{X} = \frac{\mu}{\Theta}\boldsymbol{v} + \boldsymbol{K}_0, \tag{14}$$

where $\boldsymbol{K}_0 = (K_{0,1}, K_{0,2}, 0)^{\mathrm{T}}$, with T denoting transposition, is an arbitrary integration vectorial constant, thus showing that the velocity hodograph of the Kepler problem is a circumference of radius μ/Θ and origin $\boldsymbol{K}_0$, cf. [97]. Now, plugging Equation (14) into Equation (3), we readily obtain

$$\boldsymbol{e} = \frac{\Theta}{\mu}\boldsymbol{K}_0 \times \boldsymbol{n}, \tag{15}$$

from which

$$\boldsymbol{K}_0 = \frac{\mu}{\Theta}\boldsymbol{n} \times \boldsymbol{e}. \tag{16}$$

Therefore, the decomposition in Equation (14) splits the velocity of the Kepler problem into one component orthogonal to the radius of constant modulus μ/Θ and another (constant) component orthogonal to the eccentricity vector and modulus $e\mu/\Theta$, with $e = \|\boldsymbol{e}\|$ denoting the eccentricity of the orbit, cf. [98]. Namely

$$\boldsymbol{X} = \frac{\mu}{\Theta}(\boldsymbol{v} + \boldsymbol{n} \times \boldsymbol{e}). \tag{17}$$

This classical decomposition is illustrated in Figure 2 in reference to the orbit.

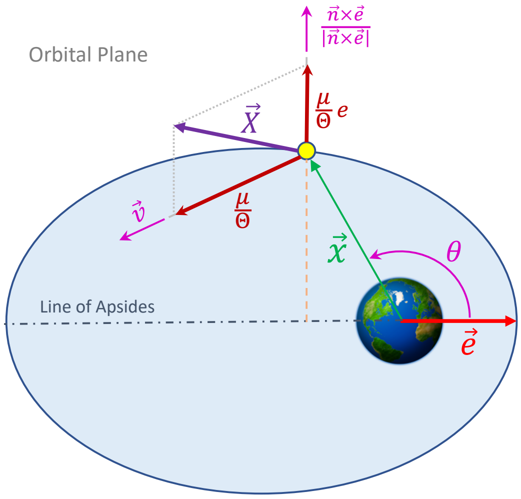

Figure 2. Velocity decomposition in Equation (17).

Therefore, the velocity hodograph of the Kepler problem is determined as a function of the polar angle and three constant, scalar velocities. That is, $\boldsymbol{X} = \boldsymbol{X}(\theta; C, S, \zeta_3)$, where the velocities

$$C = +\frac{\mu}{\Theta}(\boldsymbol{n} \times \boldsymbol{e}) \cdot \boldsymbol{v}^* = \frac{\mu}{\Theta}\boldsymbol{e} \cdot \boldsymbol{u}^*, \tag{18}$$

$$S = -\frac{\mu}{\Theta}(\boldsymbol{n} \times \boldsymbol{e}) \cdot \boldsymbol{u}^* = \frac{\mu}{\Theta}\boldsymbol{e} \cdot \boldsymbol{v}^*, \tag{19}$$

$$\zeta_3 = \frac{\mu}{\Theta}, \tag{20}$$

have been repeatedly pointed out as insightful parameters regarding astrodynamics applications [99–101]—yet their evident geometric character was not always clearly recognized [92,102–104]. The geometry of the velocity hodograph is illustrated in Figure 3, showing the relevant scalar and vectorial components of the velocity.

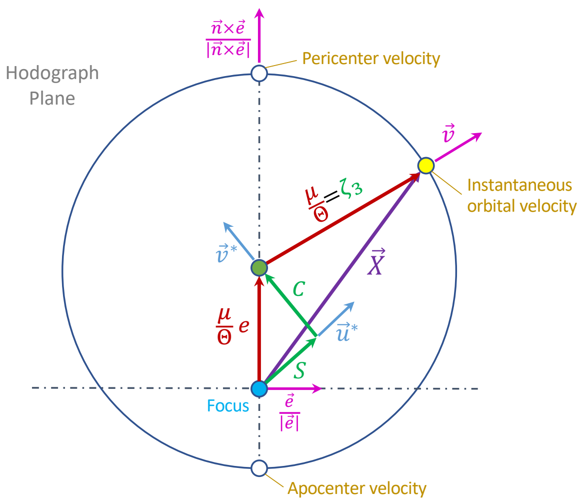

Figure 3. Velocity hodograph showing the components of $\boldsymbol{X}$ in Equations (3) and (18)–(20).

2.3. The Keplerian Orbit in Terms of the Hodographic Constants

Replacing $\boldsymbol{X}$ from Equation (11) and $\boldsymbol{G}$ from Equation (2) into Equation (3) and multiplying it scalarly by $\boldsymbol{u}$, we readily obtain the conic equation that materializes the orbit of the Kepler problem

$$\boldsymbol{e} \cdot \boldsymbol{u} = \frac{p}{r} - 1, \tag{21}$$

where $p = \Theta^2/\mu$ is the parameter of the conic. Differentiation of Equation (21) with respect to time yields

$$-\frac{\Theta}{\mu}\frac{\Theta}{r^2}\frac{\mathrm{d}r}{\mathrm{d}t} = \boldsymbol{e} \cdot \frac{\mathrm{d}\boldsymbol{u}}{\mathrm{d}t},$$

from which, on account of Equation (10), we obtain

$$R = -\frac{\mu}{\Theta}\boldsymbol{e} \cdot \boldsymbol{v}. \tag{22}$$

Now, plugging Equation (4) into Equation (21) and taking Equations (18)–(20) into account, we obtain

$$\frac{p}{r} = 1 + \frac{1}{\zeta_3}(C\cos\theta + S\sin\theta), \tag{23}$$

thus disclosing the harmonic character of the inverse of the distance on a time scale proportional to θ. Analogously, replacing Equation (5) into Equation (22), we obtain

$$R = C\sin\theta - S\cos\theta. \tag{24}$$

The Cartesian coordinates are then recovered from the canonical set of polar variables (r, θ, R, Θ) by means of standard transformations.

3. The Basic Set of Ideal Elements for Perturbed Kepler Motion

Beyond the integrable Kepler problem, the Newtonian equations of perturbed Keplerian motion are written in the form

$$\frac{\mathrm{d}\boldsymbol{x}}{\mathrm{d}t} = \boldsymbol{X}, \tag{25}$$

$$\frac{\mathrm{d}\boldsymbol{X}}{\mathrm{d}t} = -\frac{\mu}{r^3}\boldsymbol{x} + \boldsymbol{P}, \tag{26}$$

where the perturbation of the Keplerian acceleration $\boldsymbol{P}$ depends, in general, on position, velocity, and time. For given initial conditions $\boldsymbol{x}_0 \equiv \boldsymbol{x}(t_0)$, $\boldsymbol{X}_0 \equiv \boldsymbol{X}(t_0)$, the solution to Equations (25) and (26) is unique and can always be obtained by numerical methods.

Alternatively to the numerical integration in Cartesian coordinates, the integration of *elements* can be advantageous. They are defined such that their variations remain constant in unperturbed Keplerian motion. Therefore, it is expected that their variations under small perturbations change only slowly for *constant elements*, like the semimajor axis or the epoch of periapsis passage, or almost linearly in the case of *linear elements* like the mean anomaly.

Obviously the angular momentum vector and the eccentricity vector are constant elements of the Keplerian motion, whose variations under perturbations are obtained from differentiation of Equations (2) and (3). For the first, taking Equation (26) into account, we obtain

$$\frac{\mathrm{d}\boldsymbol{G}}{\mathrm{d}t} = r\boldsymbol{u} \times \boldsymbol{P}, \tag{27}$$

from which, on account of the identity $\Theta\,\mathrm{d}\Theta/\mathrm{d}t = \boldsymbol{G} \cdot \mathrm{d}\boldsymbol{G}/\mathrm{d}t$, we readily obtain

$$\frac{\mathrm{d}\Theta}{\mathrm{d}t} = r(\boldsymbol{P} \cdot \boldsymbol{v}). \tag{28}$$

Moreover, replacing $\boldsymbol{G} = \Theta\boldsymbol{n}$ and $\boldsymbol{u} \times \boldsymbol{P} = (\boldsymbol{P} \cdot \boldsymbol{v})\boldsymbol{n} - (\boldsymbol{P} \cdot \boldsymbol{n})\boldsymbol{v}$ in Equation (27) and solving the resulting equation for the variation of $\boldsymbol{n}$, in which Equation (28) is, in turn, replaced, we obtain

$$\frac{\mathrm{d}\boldsymbol{n}}{\mathrm{d}t} = -\frac{r}{\Theta}(\boldsymbol{P} \cdot \boldsymbol{n})\boldsymbol{v}, \tag{29}$$

and hence, replacing Equations (10) and (29) for the variation of $\boldsymbol{v} = \boldsymbol{n} \times \boldsymbol{u}$,

$$\frac{\mathrm{d}\boldsymbol{v}}{\mathrm{d}t} = \frac{r}{\Theta}(\boldsymbol{P} \cdot \boldsymbol{n})\boldsymbol{n} - \frac{\Theta}{r^2}\boldsymbol{u}. \tag{30}$$

On the other hand, the variation of the eccentricity vector is computed using Equations (10), (26), and (27) to obtain

$$\frac{\mathrm{d}\boldsymbol{e}}{\mathrm{d}t} = \frac{\Theta}{\mu}\boldsymbol{P} \times \boldsymbol{n} + \frac{r}{\mu}\boldsymbol{X} \times (\boldsymbol{u} \times \boldsymbol{P}). \tag{31}$$

Different combinations of the components of the basic vectorial integrals give rise to constant elements, too. This is the particular case of the three velocities that characterize the Keplerian hodograph in Equations (18)–(20), whose definitions only require algebraic operations between the components of the eccentricity vector and the unit vectors defining the reference frame (all of them being constant in the Keplerian approximation). It is also the case of the variables determining the orientation of the reference frame with respect to the space frame, which only involve trigonometric relations between the constant vectors of the space frame and those defining the reference frame. On the contrary, since the orbital frame evolves non-linearly in general, even in the Kepler problem, the variables related to the radial distance are not elements—as becomes clear from Equations (21) and (22). Still, they are efficiently integrated on a time scale proportional to θ, a case in which the inverse of the distance is solved from a second-order, linear differential equation with constant coefficients, thus giving rise to harmonic oscillations, as follows from Equations (23) and (24). This latter case will be discussed in Section 4.

Finally, the location of the particle, either in the orbit or the hodograph, must be determined through the computation of θ, which is not an element. While this is not a major concern in the integration of lower-eccentricity orbits, replacing θ by a linear element commonly brings benefits to the solution of eccentric orbits—yet this is at the expense of losing the generality of θ in the description of any kind of conic. Still, we adhere to tradition and use the nonsingular, mean distance to the departure point like the linear element providing the timing on the ellipse.

3.1. Ideal Frames

Different choices of the reference frame, like nodal or apsidal frames, may offer different advantages. However, as already mentioned in the introduction, appealing simplifications of the equations of motion arise from the choice of *ideal* frames, in which the velocity is the same as when measured in the inertial frame. As follows from the theorem of the moving frame in Equation (6), this means that the vectorial product of $\boldsymbol{\omega}$ and $\boldsymbol{x}$ must vanish for an ideal frame, which happens only when the rotation of the reference frame takes place about the $\boldsymbol{u}$ axis of the orbital frame.

Imposing this condition to the reference frame is easily done by noting that the time variation of the orbital frame given by Equations (10), (29) and (30) can be written like the rotation [22]

$$\frac{\mathrm{d}}{\mathrm{d}t}(\boldsymbol{u}, \boldsymbol{v}, \boldsymbol{n}) = \boldsymbol{\omega} \times (\boldsymbol{u}, \boldsymbol{v}, \boldsymbol{n}), \tag{32}$$

with angular velocity

$$\boldsymbol{\omega} = \frac{r}{\Theta}(\boldsymbol{P} \cdot \boldsymbol{n})\boldsymbol{u} + \frac{\Theta}{r^2}\boldsymbol{n}. \tag{33}$$

Then, choosing a reference frame that rotates with angular velocity

$$\boldsymbol{\omega}^* = \frac{r}{\Theta}(\boldsymbol{P}\cdot\boldsymbol{n})\boldsymbol{u}, \tag{34}$$

turns it into ideal and makes the rotation from the reference to the orbital frame $\boldsymbol{\omega}_{\mathrm{K}} = \boldsymbol{\omega} - \boldsymbol{\omega}^*$ to be purely Keplerian in spite of the perturbations. Therefore, on account of Equation (4), the variation of the chosen elements that materialize the reference, ideal frame must be computed from

$$\boldsymbol{\omega}^* = \frac{r}{\Theta}(\boldsymbol{P}\cdot\boldsymbol{n})(\boldsymbol{u}^*\cos\theta + \boldsymbol{v}^*\sin\theta). \tag{35}$$

The attitude of the reference frame is customarily obtained from the Euler angles (Ω, I, β). More precisely, the inclination $0 \le I \le \pi$ between the orbital plane $\boldsymbol{n}$ and the inertial plane $\boldsymbol{k}$ is obtained from $\cos I = \boldsymbol{n}\cdot\boldsymbol{k}$. The right ascension of the ascending node $\Omega \in [0, 2\pi)$ is reckoned from $\boldsymbol{i}$ to the direction of the ascending node $\boldsymbol{\ell} = \boldsymbol{k}\times\boldsymbol{n}/\sin I$. Finally, the angle $\beta \in [0, 2\pi)$ is unambiguously determined from $\boldsymbol{\ell}\cdot\boldsymbol{u}^* = \cos\beta$, $\boldsymbol{\ell}\times\boldsymbol{u}^* = \boldsymbol{n}\sin\beta$. The triad $(\boldsymbol{\ell}, \boldsymbol{n}\times\boldsymbol{\ell}, \boldsymbol{n})$ defines the *nodal frame*.

The variation of the Euler angles under perturbations is obtained from the usual relation [105,106]

$$\boldsymbol{\omega}^* = \frac{\mathrm{d}\Omega}{\mathrm{d}t}\boldsymbol{k} + \frac{\mathrm{d}I}{\mathrm{d}t}\boldsymbol{\ell} + \frac{\mathrm{d}\beta}{\mathrm{d}t}\boldsymbol{n}, \tag{36}$$

from which, on account of Equation (35), the components $(\boldsymbol{\omega}^*\cdot\boldsymbol{u}^*, \boldsymbol{\omega}^*\cdot\boldsymbol{v}^*, \boldsymbol{\omega}^*\cdot\boldsymbol{n})$ are computed and solved for the time derivatives to obtain

$$\frac{\mathrm{d}\Omega}{\mathrm{d}t} = \frac{r}{\Theta}(\boldsymbol{P}\cdot\boldsymbol{n})\frac{\sin(\theta+\beta)}{\sin I}, \tag{37}$$

$$\frac{\mathrm{d}I}{\mathrm{d}t} = \frac{r}{\Theta}(\boldsymbol{P}\cdot\boldsymbol{n})\cos(\theta+\beta), \tag{38}$$

$$\frac{\mathrm{d}\beta}{\mathrm{d}t} = -\frac{\mathrm{d}\Omega}{\mathrm{d}t}\cos I, \tag{39}$$

which are the variations that must fulfill the reference frame to be ideal under perturbations. Note that while the initial values of Ω and I are fixed from the dynamics, the freedom in choosing the initial value of β gives rise to countless ideal frames. Usual options are to choose an initial β such that $\boldsymbol{u}^*(t_0) = \boldsymbol{u}(t_0)$ [22] or such that $\boldsymbol{u}^*(t_0)$ points to the initial pericenter [66].

3.2. HODEI Formulation

To avoid the singularities affecting Equations (37) and (39) when $I = 0$, the Euler angles are conveniently replaced by the nonsingular, redundant set of Euler parameters

$$\lambda_1 = \sin\tfrac{1}{2}I\cos\tfrac{1}{2}(\Omega-\beta), \tag{40}$$

$$\lambda_2 = \sin\tfrac{1}{2}I\sin\tfrac{1}{2}(\Omega-\beta), \tag{41}$$

$$\lambda_3 = \cos\tfrac{1}{2}I\sin\tfrac{1}{2}(\Omega+\beta), \tag{42}$$

$$\lambda_4 = \cos\tfrac{1}{2}I\cos\tfrac{1}{2}(\Omega+\beta), \tag{43}$$

which are linked by the geometric constraint $\sum_{j=1}^{4}\lambda_j^2 = 1$. The variations of the Euler parameters are then computed by differentiation of Equations (40)–(43) and the consequent replacement of Equations (37)–(39). Straightforward computations yield

$$\frac{\mathrm{d}\boldsymbol{\lambda}}{\mathrm{d}t} = \frac{r}{2\Theta}(\boldsymbol{P}\cdot\boldsymbol{n})\begin{pmatrix} \mathbf{0}_2 & \mathbf{m} \\ -\mathbf{m} & \mathbf{0}_2 \end{pmatrix}\boldsymbol{\lambda}, \tag{44}$$

where $\boldsymbol{\lambda} = (\lambda_1, \lambda_2, \lambda_3, \lambda_4)^{\mathrm{T}}$, $\mathbf{0_2}$ denotes the null matrix of rank 2, and, assuming vectors as columns of a matrix, $\mathbf{m} = (\boldsymbol{u}^*, \boldsymbol{v}^*)^{\mathrm{T}}(\boldsymbol{v}, \boldsymbol{u})$. That is, from Equations (4) and (5),

$$\mathbf{m} = \begin{pmatrix} \boldsymbol{u}^* \cdot \boldsymbol{v} & \boldsymbol{u}^* \cdot \boldsymbol{u} \\ \boldsymbol{v}^* \cdot \boldsymbol{v} & \boldsymbol{v}^* \cdot \boldsymbol{u} \end{pmatrix} = \begin{pmatrix} -\sin\theta & \cos\theta \\ \cos\theta & \sin\theta \end{pmatrix}. \tag{45}$$

Equation (44) comprises the differential equations that describe the attitude of the ideal reference frame without any singularity. That the Euler parameters are elements is obvious from the vanishing of their variations in the absence of perturbations.

Tracking the slow variation of the hodograph under perturbations requires differentiation of the velocities in Equations (18)–(20). The variation of ζ_3 is unrelated to the ideal frame and is trivially obtained from Equation (28) as

$$\frac{\mathrm{d}\zeta_3}{\mathrm{d}t} = -\frac{\zeta_3^2}{\mu} r(\boldsymbol{P} \cdot \boldsymbol{v}). \tag{46}$$

On the contrary, the computation of the variations of C and S must adhere to the ideal-frame definition and requires slightly more-involved computations, which we summarize from [22] (see also [82]).

From their definition in Equations (18) and (19), we may write $C\boldsymbol{u}^* + S\boldsymbol{v}^* = (\mu/\Theta)\boldsymbol{e}$, whose differentiation in the rotating, ideal frame yields

$$\frac{\mathrm{d}C}{\mathrm{d}t}\boldsymbol{u}^* + \frac{\mathrm{d}S}{\mathrm{d}t}\boldsymbol{v}^* = -\frac{\mu}{\Theta^2}\frac{\mathrm{d}\Theta}{\mathrm{d}t}\boldsymbol{e} + \frac{\mu}{\Theta}\left(\frac{\mathrm{d}\boldsymbol{e}}{\mathrm{d}t}\right)_{\omega^*},$$

where we replace the variation of Θ from Equation (28) and $\boldsymbol{e}$ from Equation (3), in which $\boldsymbol{X}$ is, in turn, replaced from Equation (11). Straightforward operations yield

$$\frac{\mathrm{d}C}{\mathrm{d}t}\boldsymbol{u}^* + \frac{\mathrm{d}S}{\mathrm{d}t}\boldsymbol{v}^* = \frac{\mu}{\Theta}\left(\frac{\mathrm{d}\boldsymbol{e}}{\mathrm{d}t}\right)_{\omega^*} + (\boldsymbol{P} \cdot \boldsymbol{v})\left[\left(\frac{r}{p} - 1\right)\boldsymbol{u} + \frac{rR}{\Theta}\boldsymbol{v}\right],$$

and hence,

$$\frac{\mathrm{d}C}{\mathrm{d}t} = \frac{\mu}{\Theta}\boldsymbol{u}^* \cdot \left(\frac{\mathrm{d}\boldsymbol{e}}{\mathrm{d}t}\right)_{\omega^*} + (\boldsymbol{P} \cdot \boldsymbol{v})\left[\left(\frac{r}{p} - 1\right)\boldsymbol{u} \cdot \boldsymbol{u}^* + \frac{rR}{\Theta}\boldsymbol{v} \cdot \boldsymbol{u}^*\right], \tag{47}$$

$$\frac{\mathrm{d}S}{\mathrm{d}t} = \frac{\mu}{\Theta}\boldsymbol{v}^* \cdot \left(\frac{\mathrm{d}\boldsymbol{e}}{\mathrm{d}t}\right)_{\omega^*} + (\boldsymbol{P} \cdot \boldsymbol{v})\left[\left(\frac{r}{p} - 1\right)\boldsymbol{u} \cdot \boldsymbol{v}^* + \frac{rR}{\Theta}\boldsymbol{v} \cdot \boldsymbol{v}^*\right]. \tag{48}$$

The derivative of the eccentricity vector in the rotating frame is now computed from Equation (31) using the theorem of the moving frame. That is, $(\mathrm{d}\boldsymbol{e}/\mathrm{d}t)_{\omega^*} = \mathrm{d}\boldsymbol{e}/\mathrm{d}t - \boldsymbol{\omega}^* \times \boldsymbol{e}$, where we replace Equations (3) and (34) in the cross product of $\boldsymbol{\omega}^*$ and $\boldsymbol{e}$ to obtain

$$\left(\frac{\mathrm{d}\boldsymbol{e}}{\mathrm{d}t}\right)_{\omega^*} = \frac{\Theta}{\mu}\boldsymbol{P} \times \boldsymbol{n} + \frac{r}{\mu}\boldsymbol{X} \times (\boldsymbol{u} \times \boldsymbol{P}) - \frac{r}{\mu}(\boldsymbol{P} \cdot \boldsymbol{n})\boldsymbol{u} \times (\boldsymbol{X} \times \boldsymbol{n}), \tag{49}$$

in which we further replace $\boldsymbol{X}$ from Equation (11), and $\boldsymbol{P} = (\boldsymbol{P} \cdot \boldsymbol{u})\boldsymbol{u} + (\boldsymbol{P} \cdot \boldsymbol{v})\boldsymbol{v} + (\boldsymbol{P} \cdot \boldsymbol{n})\boldsymbol{n}$. Hence,

$$\left(\frac{\mathrm{d}\boldsymbol{e}}{\mathrm{d}t}\right)_{\omega^*} = \frac{\Theta}{\mu}\left[(\boldsymbol{P} \cdot \boldsymbol{v})\left(2\boldsymbol{u} - \frac{rR}{\Theta}\boldsymbol{v}\right) - (\boldsymbol{P} \cdot \boldsymbol{u})\boldsymbol{v}\right], \tag{50}$$

which is, in turn, replaced into Equations (47) and (48) using Equation (45) to yield

$$\frac{\mathrm{d}C}{\mathrm{d}t} = (\boldsymbol{P} \cdot \boldsymbol{v})\left(\frac{r}{p} + 1\right)\cos\theta + (\boldsymbol{P} \cdot \boldsymbol{u})\sin\theta, \tag{51}$$

$$\frac{\mathrm{d}S}{\mathrm{d}t} = (\boldsymbol{P} \cdot \boldsymbol{v})\left(\frac{r}{p} + 1\right)\sin\theta - (\boldsymbol{P} \cdot \boldsymbol{u})\cos\theta. \tag{52}$$

The variations of the *ideal elements* $(C, S, \zeta_3, \lambda_1, \lambda_2, \lambda_3, \lambda_4)$ is what we call the HODEI formulation—for **hod**ographic, **E**uler parameters, **i**deal-frame formulation—and is customary in the literature with minor modifications [22].[1] Still, to integrate the solution for given initial conditions, we need to know θ as a function of time. This can be achieved by complementing the differential system with the variation of θ, as given in Equation (9), which can be rewritten as

$$\frac{\mathrm{d}\theta}{\mathrm{d}t} = \frac{\mu}{r^2\zeta_3} = \frac{\zeta_3^3}{\mu}\frac{p^2}{r^2}. \tag{53}$$

3.3. The Timing on the Osculating Ellipse

Recall that the radius is replaced in terms of the ideal elements and the polar angle in the above equations using Equation (23). Thus, Equation (53) can be written as

$$\frac{\mathrm{d}\theta}{\mathrm{d}t} = \frac{\zeta_3^3}{\mu}\left[1 + \frac{1}{\zeta_3}(C\cos\theta + S\sin\theta)\right]^2. \tag{54}$$

which clearly shows that, while C, S, and ζ_3 are constant in the Keplerian case, θ evolves non-linearly with time at a rate given by the variation of the true anomaly $f = \theta - \omega$, where ω denotes the argument of the periapsis reckoned from the departure point. Therefore, θ is not an element. On the contrary, the variation of the mean distance from the departure point $F = M + \omega$, with M denoting the mean anomaly, is certainly an element of the perturbed Keplerian motion. This becomes obvious from its definition and the fact that

$$M = n(t - t_{\mathrm{P}}), \tag{55}$$

with constant mean motion n and time of periapsis passage t_{P} for pure Keplerian motion.

Let us check this fact in the context of the ideal-frame formulation, too. The variation of F in terms of the hodographic elements is thoroughly derived in Section 4 of [22], from which we directly borrow its Equation (101). Namely,

$$\frac{\mathrm{d}F}{\mathrm{d}t} = \frac{(2Q)^{3/2}}{\mu} + \frac{1}{1+\eta}\frac{1}{\zeta_3^2}\left(C\frac{\mathrm{d}S}{\mathrm{d}t} - S\frac{\mathrm{d}C}{\mathrm{d}t}\right) + 2\frac{\eta}{\mu}r\zeta_3\left(\frac{\mathrm{d}S}{\mathrm{d}t}\cos\theta - \frac{\mathrm{d}C}{\mathrm{d}t}\sin\theta\right), \tag{56}$$

where $\eta = (1 - e^2)^{1/2}$, whereas $Q = \mu/(2a)$ is the positive Keplerian energy, with a denoting the orbit semimajor axis. More precisely, from Equations (18) and (19), the components of the eccentricity vector in the ideal reference frame are

$$\boldsymbol{e}\cdot\boldsymbol{u}^* = e\cos\omega = \frac{1}{\zeta_3}C, \qquad \boldsymbol{e}\cdot\boldsymbol{v}^* = e\sin\omega = \frac{1}{\zeta_3}S, \tag{57}$$

from which

$$\eta = \sqrt{1 - (C^2 + S^2)/\zeta_3^2}, \tag{58}$$

and hence

$$Q = \frac{\mu^2}{2\Theta^2}(1 - e^2) = \frac{1}{2}\left[\zeta_3^2 - (C^2 + S^2)\right]. \tag{59}$$

In the Keplerian case, in which C, S, ζ_3, and Q are constant, Equation (56) turns into

$$\frac{\mathrm{d}F}{\mathrm{d}t} = \frac{(2Q)^{3/2}}{\mu}, \tag{60}$$

thus clearly adhering to the definition of an orbital element.

Undeniably, the computation of the position from the ideal element F requires the solution of Kepler's equation to obtain θ at each step of the integration procedure. More precisely, we replace the eccentric anomaly u in Kepler's equation $M = u - e\sin u$ by the eccentric distance from the departure point $\psi = u + \omega$. After trigonometric expansions, we also replace the components of the eccentricity vector from Equation (57) and obtain Kepler's equation in the modified form

$$F = \psi - \frac{1}{\zeta_3}(C\sin\psi - S\cos\psi), \tag{61}$$

cf. [108]. Once ψ has been computed from Equation (61), we use the standard relations of the ellipse $r\cos f = a(\cos u - e)$, $r\sin f = a\eta\sin u$, in which we replace the true anomaly f by $f = \theta - \omega$ and the eccentric one by $u = \psi - \omega$ to obtain

$$\frac{r}{a}\cos\theta = \cos\psi - \frac{1}{\zeta_3}\left(C - \frac{\psi - F}{1+\eta}S\right), \tag{62}$$

$$\frac{r}{a}\sin\theta = \sin\psi - \frac{1}{\zeta_3}\left(S + \frac{\psi - F}{1+\eta}C\right), \tag{63}$$

which are Equations (84) and (85) of [22] and from which the in-track angle θ is determined without ambiguity.

3.4. Initialization

The initial ideal elements needed to launch the propagation are readily obtained from the Cartesian coordinates $\boldsymbol{x}_0 = \boldsymbol{x}(t_0)$, $\boldsymbol{X}_0 = \boldsymbol{X}(t_0)$. Thus, we first compute $r_0 = \|\boldsymbol{x}_0\|$ and $\boldsymbol{G}_0 = \boldsymbol{x}_0 \times \boldsymbol{X}_0$, from which

$$\Theta_0 = \|\boldsymbol{G}_0\|. \tag{64}$$

Hence, $\boldsymbol{u}_0 = \boldsymbol{x}_0/r_0$, $\boldsymbol{n}_0 = \boldsymbol{G}_0/\Theta_0$, and $\boldsymbol{v}_0 = \boldsymbol{n}_0 \times \boldsymbol{u}_0$. Next, the Euler parameters are obtained from the standard relations [109,110]

$$\lambda_{4,0} = \frac{1}{2}(1 + \boldsymbol{u}_0\cdot\boldsymbol{i} + \boldsymbol{v}_0\cdot\boldsymbol{j} + \boldsymbol{n}_0\cdot\boldsymbol{k})^{1/2}, \quad \begin{pmatrix} \lambda_{1,0} \\ \lambda_{2,0} \\ \lambda_{3,0} \end{pmatrix} = \frac{1}{4\lambda_{4,0}}\begin{pmatrix} \boldsymbol{v}_0\cdot\boldsymbol{k} - \boldsymbol{n}_0\cdot\boldsymbol{j} \\ \boldsymbol{n}_0\cdot\boldsymbol{i} - \boldsymbol{u}_0\cdot\boldsymbol{k} \\ \boldsymbol{u}_0\cdot\boldsymbol{j} - \boldsymbol{v}_0\cdot\boldsymbol{i} \end{pmatrix}. \tag{65}$$

Finally, for

$$\theta_0 = 0, \tag{66}$$

and on account of $\boldsymbol{e}_0 = (1/\mu)\boldsymbol{X}_0 \times \boldsymbol{G}_0 - \boldsymbol{u}_0$, we compute

$$\begin{array}{rcccl} \zeta_{3,0} & = & \mu/\Theta_0, & & \\ C_0 & = & \zeta_{3,0}\boldsymbol{u}_0\cdot\boldsymbol{e}_0 & = & \boldsymbol{X}_0\cdot\boldsymbol{v}_0 - \zeta_{3,0}, \\ S_0 & = & \zeta_{3,0}\boldsymbol{v}_0\cdot\boldsymbol{e}_0 & = & -\boldsymbol{u}_0\cdot\boldsymbol{X}_0. \end{array} \tag{67}$$

Ephemeris at the event $t = t_i$ are obtained from the polar variables in the orbital plane (r, θ, R, Θ), where $r(t_i)$ is computed from Equation (23), $\theta(t_i)$ is solved from Equations (62) and (63), $R(t_i)$ is obtained from Equation (24), and $\Theta(t_i) = \mu/\zeta_3(t_i)$. Then,

$$\boldsymbol{x} = \mathcal{M}\begin{pmatrix} r\cos\theta \\ r\sin\theta \\ 0 \end{pmatrix}, \qquad \boldsymbol{X} = \mathcal{M}\begin{pmatrix} R\cos\theta - (\Theta/r)\sin\theta \\ R\sin\theta + (\Theta/r)\cos\theta \\ 0 \end{pmatrix}, \tag{68}$$

where

$$\mathcal{M} = \begin{pmatrix} 1 - 2(\lambda_2^2 + \lambda_3^2) & 2(\lambda_1\lambda_2 - \lambda_4\lambda_3) & 2(\lambda_1\lambda_3 + \lambda_2\lambda_4) \\ 2(\lambda_1\lambda_2 + \lambda_4\lambda_3) & 1 - 2(\lambda_1^2 + \lambda_3^2) & 2(\lambda_2\lambda_3 - \lambda_1\lambda_4) \\ 2(\lambda_1\lambda_3 - \lambda_2\lambda_4) & 2(\lambda_2\lambda_3 + \lambda_1\lambda_4) & 1 - 2(\lambda_1^2 + \lambda_2^2) \end{pmatrix}, \tag{69}$$

is the rotation matrix from the ideal to the space frame.

Alternatively, the use of a fixed *departure frame* matching the orbital frame at the starting time may help in preventing the loss of significant digits along the numerical integration. This is the case for high-inclination orbits, whose inclination variations are tracked with only a few significant digits in the space frame but are integrated with full accuracy when referred to the departure frame, in which the inclination remains close to zero [22,63,64,82]. In that case, Equation (68), which now denotes the coordinates in the departure frame, is further referred to the space frame by a constant, additional rotation.

4. Time Transformation and Fictitious-Time Elements

Alternatively to the classical integration of the physical-time variations, it may be advantageous to carry out the integration in a fictitious time ς, defined by the time transformation

$$\mathrm{d}t = c_\alpha r^\alpha \mathrm{d}\varsigma, \tag{70}$$

where α is a positive, numeric constant, and the coefficient c_α may depend on the chosen set of coordinates or elements as well as on the total energy—whether it is constant or not [6,77].

4.1. Laplace's Time-Regularization

In particular, for $\alpha = 2$, the customary change stemming from the fundamental relation Equation (9)

$$\mathrm{d}t = \frac{r^2 \zeta_3}{\mu} \mathrm{d}\theta, \tag{71}$$

sets the ideal-frame variations in the convenient form

$$\frac{\mathrm{d}\boldsymbol{\lambda}}{\mathrm{d}\theta} = \frac{1}{2}(\boldsymbol{P}^* \cdot \boldsymbol{n}) \begin{pmatrix} \mathbf{0}_2 & \mathbf{m} \\ -\mathbf{m} & \mathbf{0}_2 \end{pmatrix} \boldsymbol{\lambda}, \tag{72}$$

$$\frac{\mathrm{d}C}{\mathrm{d}\theta} = \frac{\mu}{r\zeta_3}\left[(\boldsymbol{P}^* \cdot \boldsymbol{v})\left(\frac{r}{p} + 1\right)\cos\theta + (\boldsymbol{P}^* \cdot \boldsymbol{u})\sin\theta\right], \tag{73}$$

$$\frac{\mathrm{d}S}{\mathrm{d}\theta} = \frac{\mu}{r\zeta_3}\left[(\boldsymbol{P}^* \cdot \boldsymbol{v})\left(\frac{r}{p} + 1\right)\sin\theta - (\boldsymbol{P}^* \cdot \boldsymbol{u})\cos\theta\right], \tag{74}$$

$$\frac{\mathrm{d}\zeta_3}{\mathrm{d}\theta} = -\,\zeta_3(\boldsymbol{P}^* \cdot \boldsymbol{v}), \tag{75}$$

$$\frac{\mathrm{d}t}{\mathrm{d}\theta} = \frac{r^2\zeta_3}{\mu}, \tag{76}$$

where we abbreviated $\boldsymbol{P}^* = \boldsymbol{P} r^3 \zeta_3^2/\mu^2$, thus making the perturbation non-dimensional.[2]

The improvements to the simple and effective time-regularization given by Equation (71) result into a dramatic accuracy increase for the integration of the geometric coordinates of the orbit. However, the time transformation does not change the Keplerian dynamics and simply gathers the Lyapunov-type instabilities into the integration of the physical time from Equation (76). The errors in the timing stemming from this fact produce a lack of synchronism between the computed and the true solution that may result in analogous ephemeris errors to those obtained when the integration is carried out using the physical time as the independent variable.

We remark that the definition of elements widely applies to the integration in a fictitious time without constraint to the physical-time integration [6]. That the physical-time variable is not an element of the fictitious-time integration is readily checked from Equation (76) in the same way as we already did in Equation (54). Therefore, replacing the direct integration of the physical time by the integration of a fictitious-time element followed by the computation of the physical time from the time-element definition could bring additional benefits to the integration process [6,43,84,85]. Among the different possibilities, elements related to the time of periapsis passage t_P are natural choices for *constant* time elements, which we inherit from traditional formulations of the variation-of-parameters method by astronomers [10,111]. Alternatively, the integration of the physical time can be replaced by a *linear* time element of the form $\tau = t_\mathrm{P} + n\varsigma$, which in the Keplerian approximation evolves linearly in the fictitious time ς with frequency $n = (2Q)^{3/2}/\mu$. In the end, the fictitious time must be recovered from its relation with the time element, which is naturally established through Kepler's equation.

4.2. Time Elements

Based on the anomalies of the elliptic motion, different authors derived from Kepler's equation time elements that apply for regularized equations relying on either osculating [78,79,84] or non-osculating elements [80,90,112]. In order to avoid the singularities associated with the classical anomalies, in what follows, we derive the variation equations of analogous time-elements, which are new to our knowledge, based on the mean distance to the departure point, which is nonsingular for circular orbits.

A constant time element τ_{cons} of the fictitious-time dynamics is defined as follows. We solve the time from Equation (55) as a function of the mean anomaly and rewrite it in the form

$$t = -\frac{1}{n}(M_0 + \omega) + \frac{1}{n}(M + \omega) = \tau_{\mathrm{cons}} + \frac{\mu}{(2Q)^{3/2}}F, \tag{77}$$

where M_0 denotes the value of the mean anomaly at $t = 0$, and

$$\tau_{\mathrm{cons}} \equiv \frac{\mu}{(2Q)^{3/2}}(-F_0), \tag{78}$$

with F_0 denoting the value of F at $t = 0$. Under perturbations, τ_{cons} is no longer constant, and its fictitious-time variation is obtained by the variation-of-parameters method. That is, differentiation of Equation (77) with respect to θ yields

$$\frac{\mathrm{d}\tau_{\mathrm{cons}}}{\mathrm{d}\theta} = \frac{\mu}{(2Q)^{3/2}}\left[\frac{(2Q)^{3/2}}{\mu}\frac{\mathrm{d}t}{\mathrm{d}\theta} - \frac{\mathrm{d}F}{\mathrm{d}\theta} + \frac{3}{2}\frac{F}{Q}\frac{\mathrm{d}Q}{\mathrm{d}\theta}\right], \tag{79}$$

in which $\mathrm{d}t/\mathrm{d}\theta$ is replaced from Equation (71), the variation of the Kepler energy

$$\frac{\mathrm{d}Q}{\mathrm{d}\theta} = \zeta_3\frac{\mathrm{d}\zeta_3}{\mathrm{d}\theta} - C\frac{\mathrm{d}C}{\mathrm{d}\theta} - S\frac{\mathrm{d}S}{\mathrm{d}\theta}, \tag{80}$$

is trivially obtained from Equation (59), and, from Equation (56), $\mathrm{d}F/\mathrm{d}\theta = (r^2/\Theta)\,\mathrm{d}F/\mathrm{d}t$ results in

$$\frac{\mathrm{d}F}{\mathrm{d}\theta} = \frac{(2Q)^{3/2}}{\mu}\frac{\mathrm{d}t}{\mathrm{d}\theta} + \frac{1}{1+\eta}\frac{1}{\zeta_3^2}\left(C\frac{\mathrm{d}S}{\mathrm{d}\theta} - S\frac{\mathrm{d}C}{\mathrm{d}\theta}\right) + 2\frac{\eta}{\mu}r\zeta_3\left(\cos\theta\frac{\mathrm{d}S}{\mathrm{d}\theta} - \sin\theta\frac{\mathrm{d}C}{\mathrm{d}\theta}\right). \tag{81}$$

It is important to note that, as pointed out in [84], at each step of the numerical integration of Equation (79), the value of Q entering the above formulas should be obtained from the numerical integration of Equation (80) rather than from direct evaluation of Equation (59), where the small errors resulting from the numerical integration of ζ_3, etc. would be multiplied by twice their respective values, thus increasing the error in the determination of Q.

Alternatively, for a linear time element τ_{lin}, we rewrite Equation (77) as

$$t = \tau_{\mathrm{lin}} + \frac{\mu}{(2Q)^{3/2}}(F - \theta), \tag{82}$$

where

$$\tau_{\mathrm{lin}} \equiv \frac{\mu}{(2Q)^{3/2}}(\theta - F_0), \tag{83}$$

evolves linearly with θ in the Keplerian case. Therefore, τ_{lin} fits the definition of a (fictitious) time element, from which the physical time is recovered through Equation (82). Now, under perturbations, differentiation of Equation (82) with respect to the fictitious time θ yields

$$\frac{\mathrm{d}\tau_{\text{lin}}}{\mathrm{d}\theta} = \frac{\mu}{(2Q)^{3/2}}\left[1 + \frac{(2Q)^{3/2}}{\mu}\frac{\mathrm{d}t}{\mathrm{d}\theta} - \frac{\mathrm{d}F}{\mathrm{d}\theta} + \frac{3}{2}\frac{F-\theta}{Q}\frac{\mathrm{d}Q}{\mathrm{d}\theta}\right], \tag{84}$$

in which, again, $\mathrm{d}t/\mathrm{d}\theta$ is replaced from Equation (71), whereas the variations of the Keplerian energy Q and the mean distance to the departure point F are the same as those given in Equations (80) and (81), respectively.

Needless to say, both time elements τ_{cons} and τ_{lin} are free from singularities related to circular orbits since the direct computation of F from the (nonsingular) polar coordinates, which is needed at each integration step in order to evaluate Equation (84), is straightforward. Thus, proceeding analogously as we did in the previous derivation of Equations (62) and (63), we readily obtain

$$\frac{r}{a}\cos\theta = \cos\psi + \frac{1-\eta}{\eta}\frac{r}{a}\sin f\sin\omega - e\cos\omega, \tag{85}$$

$$\frac{r}{a}\sin\theta = \sin\psi - \frac{1-\eta}{\eta}\frac{r}{a}\sin f\cos\omega - e\sin\omega, \tag{86}$$

from which, recalling that $R = (\Theta/p)e\sin f$ from Equation (22), we can compute ψ without ambiguity from

$$\cos\psi = \frac{r\zeta_3^2}{\mu}\eta^2\cos\theta + \frac{C}{\zeta_3} - \frac{\eta}{1+\eta}\frac{rR}{\mu}S, \tag{87}$$

$$\sin\psi = \frac{r\zeta_3^2}{\mu}\eta^2\sin\theta + \frac{S}{\zeta_3} + \frac{\eta}{1+\eta}\frac{rR}{\mu}C, \tag{88}$$

where r and R are replaced from Equations (23) and (24), respectively, and η is from Equation (58). Finally, F is obtained by simple evaluation of Equation (61). Alternatively, the dimension of the differential system can be augmented with the variation of F in Equation (81), whose computation is, in fact, an unavoidable step in the evaluation of the fictitious-time element in Equation (84). Then, Equations (87) and (88) only need to be evaluated once at $\theta = 0$ to compute the initial value F_0.

We remark that the computation of ephemeris from the regularized differential equations requires the interpolation of the physical time from the numerical integration.

4.3. ORBELTI Formulation

Replacing Equation (76) with either Equation (79) or Equation (84) results in a time-regularized system of elements, as desired. On the other hand, computing the orbit from this differential system requires, in addition, recovery of the radial coordinates from the hodograph velocities and the regularized time, which is done using Equations (23) and (24). However, as already mentioned in Section 3, it so happens that in the fictitious time θ, both the inverse of the distance and the radial velocity are subject to harmonic oscillations, which are efficiently also integrated under perturbations. Therefore, the computation of the hodographic velocities C and S is optional, and we can abbreviate calculations by directly integrating the orbital coordinates. That is, calling $s = 1/r$ and using Equations (23) and (24), we readily obtain

$$\frac{\mathrm{d}s}{\mathrm{d}\theta} = -\frac{\zeta_3}{\mu}R. \tag{89}$$

A new differentiation of Equation (89) in fictitious time after replacing R from Equation (24), taking Equations (73)–(75) into account, and again making use of Equations (23) and (24), after straightforward simplifications, yields

$$\frac{\mathrm{d}^2 s}{\mathrm{d}\theta^2} + s = \frac{\zeta_3^2}{\mu} - (\boldsymbol{P}^* \cdot \boldsymbol{u})s - (\boldsymbol{P}^* \cdot \boldsymbol{v})\frac{\mathrm{d}s}{\mathrm{d}\theta}, \tag{90}$$

which is the equation of a perturbed harmonic oscillator—cf. Equation (15) on p. 70 of [63] with typos amended or Equation (70) on p. 145 of [82].

The differential system made of Equations (72), (75), (76) and (90), where the latter now reads $\mathrm{d}t/\mathrm{d}\theta = \zeta_3/(s^2\mu)$ and $\boldsymbol{P}^* = \boldsymbol{P}\zeta_3^2/(s^3\mu^2)$, is what we call the ORBELTI formulation—for **orb**ital, **E**uler parameters, **L**aplace **t**ime-regularized, **i**deal-frame formulation. It was originally proposed in [63] (see also [64]) under the "pirq" denomination with the only change being the replacement of the fictitious-time integration of the hodographic velocity ζ_3 with that of the angular momentum Θ. Variants of the ideal-frame formulation in the framework of projective decomposition using different time transformations have been proposed in [113].

5. Alternative Formulations

An elementary arrangement of the Euler parameters was later proposed in [82] and applies to both ideal-frame variants: either based on pinpointing the eccentricity vector in the ideal frame or in the linearization of the differential equation of the radial distance. The reformulation consists of replacing the standard Euler parameters λ_i, $i = 1\ldots 4$ by their modified version $g_i = \sqrt{\Theta}\,\lambda_i$ (see also [81]). In this way, the integration of Equation (72) is replaced with the integration of the variations

$$\frac{\mathrm{d}\mathbf{g}}{\mathrm{d}\theta} = \frac{1}{2}(\boldsymbol{P}^*\cdot\boldsymbol{v})\mathbf{g} + \frac{1}{2}(\boldsymbol{P}^*\cdot\boldsymbol{n})\begin{pmatrix} \mathbf{0}_2 & \mathbf{m} \\ -\mathbf{m} & \mathbf{0}_2 \end{pmatrix}\mathbf{g}, \qquad \mathbf{g} = (g_1, g_2, g_3, g_4)^{\mathrm{T}}; \tag{91}$$

cf. Equations (65)–(68) of [82].

The evaluation of Equation (91) is just slightly more demanding than that of the variations of the standard Euler parameters in Equation (72). Still, it remains competitive in a numerical integration scheme because it makes dispensable the integration of the variation of the total angular momentum in Equation (28), which now becomes a derived quantity, namely $\Theta = \sum_{i=1}^{4} g_i^2$. Therefore, the dimension of the differential system is reduced to a minimum while retaining all the merits of the ideal-frame, nonsingular formulation. Remark that at each integration step, the computational time in practical scenarios will primarily be absorbed by the evaluation of the physical model originating the perturbing acceleration rather than by the evaluation of the rest of the equation terms specific to the formulation.

Additionally, it is well-known that the incorporation of the total energy in the time transformation can be beneficial in the stabilization of the integration. This approach, which was originally taken in [77] and then followed by different authors [39,65,80], leads to the use of non-osculating elements as well as useful (non-osculating) time elements. When this latter approach is taken, the time elements discussed in Section 4 are trivially upgraded by replacing the Keplerian energy by the total energy in the trail of the time element introduced originally in [80] and re-derived here in Appendix A for completeness.

6. Conclusions

The basic approaches to the Hansen ideal-frame formulation of perturbed Keplerian motion have been briefly revisited with an emphasis on the use of osculating elements. For time-regularized formulations, we dealt fundamentally with a Sundman-type transformation that turns the true distance from the departure point—the fast, in-track variable of the ideal-frame approach—into the fictitious time of the differential equations. The use of the latter stems naturally from the classical, physical-time variation equations, which are efficiently reformulated into fictitious time when using this time transformation. More sophisticated time transformations involving the total energy and relying on the use of non-osculating variables were originally presented in the context of the canonical set of Scheifele's (true anomaly) Delaunay-similar variables, whose thorough derivation is provided as an Appendix and which we prefer to refer to as Hill-similar variables.

In the process of time-regularizing the ideal-frame variations, we derived a constant and a linear, nonsingular, fictitious-time element that are new to the best of our knowledge and may be useful for increasing the position accuracy of numerical solutions of perturbed Keplerian motion. In this task, we found notable help in the mastery of Deprit, who provided the physical-time variation of the mean distance from the departure point in terms of the ideal elements for the first time and whose seminal paper on the topic should be mandatory reading for both professors and students involved in classical celestial mechanics and astrodynamics courses.

While the discussed ideal-element formulations are mostly equivalent from a dynamical point of view and hence should be amenable for analogously efficient implementation, we did not enter the topic of which one should be preferred in the propagation of orbits pertaining to specific dynamical configurations. Certainly, the feasibility of applying simplification strategies in the transformation of an algorithm into software code is a facet of special perturbation methods that cannot be ignored in the selection of an orbit-propagation approach for particular purposes. The technicalities involved in coding the different algorithms as well as the mandatory tests that may validate them when combined with existing numerical solvers are delayed to a sequel.

Author Contributions: Conceptualization and bibliographic review, M.L. and H.U.; methodology, M.L.; funding acquisition, H.U.; writing—original draft preparation, M.L.; writing—review and editing, H.U.; Appendix, M.L. All authors have read and agreed to the published version of the manuscript.

Funding: This research was funded by the Spanish State Research Agency and the European Regional Development Fund (AEI/ERDF) grant number PID2021-123219OB-I00. The authors also acknowledge support from grant PID2020-112576GB-C22 of the same agencies and from grant TED2021-132099B-C32 funded by MCIN/AEI/10.13039/501100011033 and by "European Union NextGenerationEU/PRTR".

Informed Consent Statement: Not applicable.

Data Availability Statement: Not applicable.

Conflicts of Interest: The authors declare no conflict of interest.

Appendix A. Solution of the Kepler Problem in the Extended Phase Space

The Kepler Hamiltonian in polar canonical coordinates (r, θ, R, Θ) takes the form (see Section 4.2 of [114], for instance)

$$\mathcal{H}_{\text{Kepler}} = \frac{1}{2}\left(R^2 + \frac{\Theta^2}{r^2}\right) - \frac{\mu}{r}. \tag{A1}$$

That Θ is an integral of the Kepler problem is immediate from the ignorable character of its conjugate variable θ in Hamiltonian (A1), as follows directly from the Hamilton equations

$$\frac{\mathrm{d}(r,\theta)}{\mathrm{d}t} = \frac{\partial \mathcal{H}_{\text{Kepler}}}{\partial (R,\Theta)}, \qquad \frac{\mathrm{d}(R,\Theta)}{\mathrm{d}t} = -\frac{\partial \mathcal{H}_{\text{Kepler}}}{\partial (r,\theta)}.$$

When written in the extended phase space $(r, \theta, q, R, \Theta, Q)$, Equation (A1) turns into

$$\mathcal{H}^*_{\text{Kepler}} = \mathcal{H}_{\text{Kepler}} + Q = \frac{1}{2}\left(R^2 + \frac{\Theta^2}{r^2}\right) - \frac{\mu}{r} + Q, \tag{A2}$$

in which both θ and the time $t = q$ are ignorable coordinates, whereas the conjugate momentum to q, $Q = -\mathcal{H}_{\text{Kepler}}$, is related to the total energy. Because of that, the validity of the extended phase formulation is constrained to the manifold $\mathcal{H}^*_{\text{Kepler}} = 0$.

If, further, we carry out a transformation of the independent variable of the form

$$\mathrm{d}q \equiv \mathrm{d}t = \rho(r, \theta, q, R, \Theta, Q)\, \mathrm{d}\varsigma, \tag{A3}$$

then in the new time scale, the Keplerian flow can be derived from the new Hamiltonian

$$\widetilde{\mathcal{H}}_{\text{Kepler}} = \rho \mathcal{H}^*_{\text{Kepler}}, \tag{A4}$$

assuming that the initial conditions at $t = t_0$ match those at $\varsigma = \varsigma_0$. That is,

$$\frac{\mathrm{d}(r,\theta,q)}{\mathrm{d}\varsigma} = \frac{\partial \widetilde{\mathcal{H}}_{\text{Kepler}}}{\partial(R,\Theta,Q)}, \qquad \frac{\mathrm{d}(R,\Theta,Q)}{\mathrm{d}\varsigma} = -\frac{\partial \widetilde{\mathcal{H}}_{\text{Kepler}}}{\partial(r,\theta,q)}.$$

The interested reader is referred to [77] or Appendix A of [115] for theoretical demonstrations and additional details. We remark that, in general, ς will be non-dimensional, and hence, ρ will have dimensions of time, in which case the new Hamiltonian $\widetilde{\mathcal{H}}_{\text{Kepler}}$ will have dimensions of angular momentum instead of energy. In addition, ρ must be chosen in such a way that the new time scale increases monotonically; that is, $\rho = \mathrm{d}q/\mathrm{d}\varsigma > 0$.

We are concerned with finding a canonical transformation of variables

$$\mathcal{T} : (r,\theta,q,R,\Theta,Q) \mapsto (\lambda,g,\tau,\Lambda,G,T)$$

such that Hamiltonian (A4) becomes completely reduced to a function of only the new momenta, say

$$\widetilde{\mathcal{H}}_{\text{Kepler}} \circ \mathcal{T} = \mathcal{K}_{\text{Kepler}}(-,-,-,\Lambda,G,T). \tag{A5}$$

If the transformation $\mathcal{T}$ is found, the Kepler problem in the extended phase space is trivially integrated in the new variables. Indeed, as follows from the Hamilton equations, the new momenta Λ, G, T are constant, whereas their conjugated coordinates evolve linearly with the fictitious time. Note that this transformation will be only *weakly canonical* [116] because the complete Hamiltonian reduction will be constrained to the manifold $\widetilde{\mathcal{H}}_{\text{Kepler}} = 0$.

Appendix A.1. Family of Solutions by Hamilton–Jacobi

Due to the cyclic character of θ and q, we choose the generating function of the canonical transformation in separate variables [117]. To wit,

$$S = qT + \theta G + W(r,\Lambda,G,T). \tag{A6}$$

Therefore, the transformation equations $(R,\Theta,Q) = \partial S/\partial(r,\theta,q)$ turn into

$$Q = T, \qquad \Theta = G, \qquad R = \frac{\partial W}{\partial r}, \tag{A7}$$

and those of $(\lambda,g,\tau) = \partial S/\partial(\Lambda,G,T)$ become

$$\lambda = \frac{\partial W}{\partial \Lambda}, \qquad g = \theta + \frac{\partial W}{\partial G}, \qquad \tau = q + \frac{\partial W}{\partial T}. \tag{A8}$$

Recall that $T = Q$ is the opposite of the total energy, whereas τ has dimensions of time.

Then, plugging Equations (A7) and (A8) into Equation (A5), we form the Hamilton–Jacobi equation

$$\left[\frac{1}{2}\left(\frac{\partial W}{\partial r}\right)^2 + \frac{1}{2}\frac{G^2}{r^2} - \frac{\mu}{r} + T\right]\rho = \mathcal{K}_{\text{Kepler}}, \tag{A9}$$

which is solved for W to obtain

$$W = W(r,\Lambda,G,T) \equiv \int_{r_0}^{r} \sqrt{\chi}\,\mathrm{d}r, \tag{A10}$$

where

$$\chi = -2T + 2\frac{\mathcal{K}_{\text{Kepler}}(\Lambda,G,T)}{\rho(r,\Lambda,G,T)} + 2\frac{\mu}{r} - \frac{G^2}{r^2}. \tag{A11}$$

The lower limit r_0 is chosen as the minimum value of r for which χ vanishes, and the formal dependence of ρ on the old and new variables is a consequence of that of W. Therefore, Equations (A7) and (A8) result in the mixed transformation

$$Q = T, \tag{A12}$$
$$\Theta = G, \tag{A13}$$
$$R = \sqrt{\chi}, \tag{A14}$$
$$\lambda = \frac{\partial \mathcal{K}_{\text{Kepler}}}{\partial \Lambda} \mathcal{J}_3 - \mathcal{K}_{\text{Kepler}} \mathcal{J}_{4,\Lambda}, \tag{A15}$$
$$g = \theta + G\mathcal{J}_1 + \frac{\partial \mathcal{K}_{\text{Kepler}}}{\partial G} \mathcal{J}_3 - \mathcal{K}_{\text{Kepler}} \mathcal{J}_{4,G}, \tag{A16}$$
$$\tau = q - \mathcal{J}_2 + \frac{\partial \mathcal{K}_{\text{Kepler}}}{\partial T} \mathcal{J}_3 - \mathcal{K}_{\text{Kepler}} \mathcal{J}_{4,T}, \tag{A17}$$

in which

$$\mathcal{J}_1 = \int_{s_0}^{s} \frac{1}{\sqrt{\chi}}\, \mathrm{d}s, \qquad s = \frac{1}{r}, \tag{A18}$$
$$\mathcal{J}_2 = \int_{r_0}^{r} \frac{1}{\sqrt{\chi}}\, \mathrm{d}r, \tag{A19}$$
$$\mathcal{J}_3 = \int_{r_0}^{r} \frac{1}{\rho\sqrt{\chi}}\, \mathrm{d}r, \tag{A20}$$
$$\mathcal{J}_{4,\#} = \int_{r_0}^{r} \frac{1}{\rho^2\sqrt{\chi}} \frac{\partial \rho}{\partial \#}\, \mathrm{d}r. \tag{A21}$$

Equations (A12)–(A17) conform a *family* of canonical transformations parameterized by the functions $\mathcal{K}_{\text{Kepler}} = \mathcal{K}_{\text{Kepler}}(\Lambda, G, T)$, and $\rho = \rho(r, \Lambda, G, T)$, particular selections of which may provide useful canonical transformations of variables. In particular, there are three cases for which the integrals in Equations (A18)–(A21) enjoy solutions with elementary functions: namely, those in which $\rho = r^\alpha/\Gamma$ with $\alpha = 0, 1, 2$ and $\Gamma = \Gamma(\Lambda, G, T)$. The case $\alpha = \frac{3}{2}$ introduces the intermediate or elliptic anomalies as independent variables that are related to the true anomaly through the incomplete elliptic integral of the first kind [36,118–120].

Appendix A.2. The Hill-Similar Variables

We focus on the case $\alpha = 2$, in which

$$\rho = \frac{r^2}{\Gamma}, \tag{A22}$$

and hence, Equation (A3) becomes

$$\mathrm{d}t = \frac{r^2}{\Gamma}\, \mathrm{d}\varsigma. \tag{A23}$$

Then, plugging Equation (A22) into Equations (A20) and (A21), we readily obtain

$$\mathcal{J}_3 = -\Gamma \mathcal{J}_1, \qquad \mathcal{J}_{4,\#} = \frac{\partial \Gamma}{\partial \#} \mathcal{J}_1. \tag{A24}$$

Moreover, the choice of Γ such that the Kepler Hamiltonian becomes

$$\mathcal{K}_{\text{Kepler}} = 2(G - \Gamma), \tag{A25}$$

allows us to rearrange Equation (A11) in the convenient form [121,122]

$$\chi = -2T + 2\frac{\mu}{r} - \frac{(2\Gamma - G)^2}{r^2}. \tag{A26}$$

Therefore, Equations (A14)–(A17) turn into

$$R = \sqrt{\chi}, \tag{A27}$$

$$\lambda = -\mathcal{J}_1(G - 2\Gamma)\frac{\partial}{\partial\Lambda}(2\Gamma), \tag{A28}$$

$$g = \theta + \mathcal{J}_1(G - 2\Gamma)\left[1 - \frac{\partial}{\partial G}(2\Gamma)\right], \tag{A29}$$

$$\tau = q - \mathcal{J}_2 - \mathcal{J}_1(G - 2\Gamma)\frac{\partial}{\partial T}(2\Gamma), \tag{A30}$$

in this way reducing the parameterization of the family of canonical transformations to the single function $\Gamma = \Gamma(\Lambda, G, T)$. Moreover, since χ is quadratic in r, the still-formal indefinite integrals $\mathcal{J}_1$ and $\mathcal{J}_2$ can be solved as follows.

To integrate Equation (A18), we first rearrange Equation (A26) to the form

$$\chi = (2\Gamma - G)^2\left(\frac{1}{r} - \frac{1}{r_\mathrm{A}}\right)\left(\frac{1}{r_\mathrm{P}} - \frac{1}{r}\right). \tag{A31}$$

Next, we introduce the auxiliary functions

$$a = \frac{\mu}{2T}, \qquad p = \frac{1}{\mu}(2\Gamma - G)^2, \qquad e = \sqrt{1 - \frac{p}{a}}, \tag{A32}$$

which allow us to write the roots of Equation (A31) as either

$$\frac{1}{r_\mathrm{A}} = \frac{1-e}{p}, \qquad \frac{1}{r_\mathrm{P}} = \frac{1+e}{p}. \tag{A33}$$

or

$$r_\mathrm{A} = a(1+e), \qquad r_\mathrm{P} = a(1-e). \tag{A34}$$

Then, we change the variable

$$\frac{1}{r} = \frac{1 + e\cos f}{p}, \tag{A35}$$

from which $r_\mathrm{P} = r(f = 0)$ and $r_\mathrm{A} = r(f = \pi)$. In addition, we replace Equations (A33) and (A35) into Equation (A31), which, in turn, is replaced into Equation (A27) to obtain

$$R = \sqrt{\frac{\mu}{p}}e\sin f. \tag{A36}$$

Further, differentiation of Equation (A35) yields

$$\mathrm{d}s = \mathrm{d}(1/r) = -\frac{e}{p}\sin f\,\mathrm{d}f. \tag{A37}$$

With these changes, Equation (A18) is readily integrated in f with the lower limit $f = 0$ to obtain

$$\mathcal{J}_1 = -\frac{1}{\sqrt{\mu p}}f. \tag{A38}$$

On the other hand, replacing $\sqrt{\chi} = R$ from Equation (A27) into Equation (A19) and recalling that $R = \mathrm{d}r/\mathrm{d}t$, we obtain

$$\mathcal{J}_2 = \int_{r_\mathrm{P}}^{r} \frac{1}{R(r)}\,\mathrm{d}r = t - t_\mathrm{P}. \tag{A39}$$

That is, the difference $q - \mathcal{J}_2 = t_\mathrm{P}$ in Equation (A30) is constant and corresponds to the time of pericenter passage. Still, to compute this time, we need to solve $\mathcal{J}_2$ as a function of the polar variables. This is done with the change

$$r = a(1 - e\cos u), \tag{A40}$$

which together with the roots $r_\mathrm{P} = r(u = 0)$ and $r_\mathrm{A} = r(u = \pi)$ given in Equation (A34), are replaced in Equation (A31) to obtain χ in terms of the auxiliary variables. Straightforward computations yield

$$\frac{1}{R} = \sqrt{\frac{a}{\mu}}\frac{1 - e\cos u}{e\sin u}, \qquad \mathrm{d}r = ae\sin u\,\mathrm{d}u. \tag{A41}$$

which are plugged into Equation (A19) to trivially obtain

$$\mathcal{J}_2 = \sqrt{\frac{a^3}{\mu}}(u - e\sin u), \tag{A42}$$

and hence,

$$t_\mathrm{P} = q - \frac{\mu}{(2T)^{3/2}}(u - e\sin u), \tag{A43}$$

which is just Kepler's equation.

Therefore, Equations (A28)–(A30) turn into

$$\lambda = -f\frac{\partial}{\partial\Lambda}(2\Gamma), \tag{A44}$$

$$g = \theta + f\left[1 - \frac{\partial}{\partial G}(2\Gamma)\right], \tag{A45}$$

$$\tau = t_\mathrm{P} - f\frac{\partial}{\partial T}(2\Gamma), \tag{A46}$$

which still represent a family of transformations parameterized by $\Gamma \equiv \Gamma(G, \Lambda, T)$. Finally, we choose

$$\Gamma = G - \frac{1}{2}\left(\Lambda - \frac{\mu}{\sqrt{2T}}\right), \tag{A47}$$

which properly attaches dimensions of time to τ and assigns the role of angles to g and λ. In this way, the equations

$$\lambda = f, \tag{A48}$$

$$g = \theta - f, \tag{A49}$$

$$\tau = q - \frac{\mu}{(2T)^{3/2}}(u - e\sin u - f), \tag{A50}$$

make the (weakly) canonical transformation complete. It is worth mentioning that λ and τ can be alternatively derived from the classical Delaunay variables directly, as proposed in [123]. Note that, after [80], the time element defined by Equation (A50) has been repeatedly used to improve the accuracy of solutions to perturbed Keplerian motion based on the numerical integration of the equations of motion in a fictitious time [90,91,119].

The canonical variables $(\lambda, g, \tau, \Lambda, G, T)$ are customarily known as (true anomaly) *Delaunay-similar* or (true anomaly) DS variables [77,80,87]. However, as pointed out in [122], these variables can be obtained as an extension to space-time of Hill's original transformation that converts f into a canonical variable [124]. Therefore, we rather refer to them as *Hill-similar* variables. It goes without saying that canonical transformations pertain to geometry, and therefore, the fact that we resorted to the Kepler problem in the extended phase space to derive the Hill-similar variables does not constrain their applicability to the solution of this particular problem. On the contrary, they are successfully applied in the computation of solutions to perturbed Kepler problems [45,80].

We remark that the auxiliary variables a, p, e, f, and u used in this appendix should not be confused with the elliptic elements (osculating variables) that usually bear the same notation. Indeed, comparison of Equations (A25) and (A47) yields

$$\mathcal{K}_{\text{Kepler}} = \Lambda - \frac{\mu}{\sqrt{2T}}, \tag{A51}$$

a result that allows us to compute Γ from Equation (A25) in terms of the polar variables as follows. Because $\Theta = G$, from Equation (A13) and $\widetilde{\mathcal{H}}_{\text{Kepler}} = \mathcal{K}_{\text{Kepler}}$ from Equation (A5), we write $\Gamma = \Theta - \frac{1}{2}\widetilde{\mathcal{H}}_{\text{Kepler}}$, in which we further replace $\widetilde{\mathcal{H}}_{\text{Kepler}}$ from Equation (A4) with $\rho = r^2/\Gamma$, thus resulting in a quadratic equation for Γ. To highlight the similitude with Equation (A47), we write the solution of this quadratic equation in the form

$$\Gamma = \Theta - \frac{1}{2}\left[\Theta - r\left(2\frac{\mu}{r} - 2Q - R^2\right)^{1/2}\right], \tag{A52}$$

where the single sign of the square root stems from the Keplerian approximation $\Gamma = \Theta$. Therefore, the values of the auxiliary variables in Equation (A32) are computed in terms of the polar variables as

$$a = \frac{\mu}{2Q}, \qquad p = \frac{r^2}{\mu}\left(2\frac{\mu}{r} - R^2 - 2Q\right), \qquad e = \frac{r}{\mu}\sqrt{\left(2Q - \frac{\mu}{r}\right)^2 + 2QR^2}, \tag{A53}$$

which show their non-osculating character for perturbed Keplerian motion, in which case $Q + \frac{1}{2}(R^2 + \Theta^2/r^2) - \mu/r \neq 0$. Nevertheless, the standard relations of the ellipse $r\cos f = a(\cos u - e)$, $r\sin f = a\sqrt{1-e^2}\sin u$ still apply, as follows from the definitions of f and u in Equations (A35) and (A40), respectively.

Note that in the unperturbed case, the non-vanishing Hamilton equations stemming from Equation (A51) are

$$\frac{\mathrm{d}\lambda}{\mathrm{d}\varsigma} = \frac{\partial\mathcal{K}}{\partial\Lambda} = 1, \tag{A54}$$

$$\frac{\mathrm{d}\tau}{\mathrm{d}\varsigma} = \frac{\partial\mathcal{K}}{\partial T} = \frac{\mu}{(2T)^{3/2}}. \tag{A55}$$

Comparison of Equations (A54) and (A55) with the derivatives of Equation (A48) and Equation (A50), respectively, with respect to the new independent variable (the fictitious time) shows that $\mathrm{d}f/\mathrm{d}\varsigma = 1$, and hence, ς evolves at the same rate as the true anomaly, which is converted in this way into a canonical variable [41,87,121,122,124]. Moreover, since it evolves linearly in the new time scale, τ fits to the time-element definition [6,43,77,84]. Further, from Equation (A47) and the last of Equation (A32), we obtain $\Gamma = G = \sqrt{\mu p}$ in the Keplerian case, and the time regularization in Equation (A23) agrees with the proposal that Flury and Janin attribute to Burdet [125].

Remark that for perturbed Keplerian motion, the non-osculating angular momentum $\tilde{\Theta} = \sqrt{\mu p}$, with p replaced from Equation (A53), has been adopted in [39,65] to incorporate the total energy into the definition of the time transformation $\mathrm{d}t = (r^2/\tilde{\Theta})\,\mathrm{d}\varsigma$.

Notes

1 Note that Deprit provided much more than claimed in the conclusions of his seminal paper, where the variation of the in-track variable in the ideal frame is explicitly listed on p. 13 of [22] as Equation (96). The integration of the latter makes the solution of Kepler's equation dispensable and extends the validity of the variation equations to the integration of parabolic and hyperbolic orbits. As illustrated in [82], time-regularizing Deprit's variation equations is a trivial operation that furnishes Deprit's ideal elements (replacing the time element by the non-linearly evolving polar angle) with the same functionality as the elements derived by the Dromo software developers three decades later in [107] and further refined in [66].

2 A modified form of this differential system was proposed by the developers of the Dromo software, who referred their ideal reference to the departure apsidal frame and, as customary, dealt with the non-dimensional components of the eccentricity vector $\zeta_1 = C/\zeta_3$ and $\zeta_2 = S/\zeta_3$ instead of the hodographic velocities C and S, cf. [66]. In the fictitious time, the complexity of the differential equations is mostly analogous in both approaches. However, this is not true for the physical-time variations, where the evaluation of the differential equations $\mathrm{d}\zeta_j/\mathrm{d}t = (\zeta_3 r/\mu)\{(\boldsymbol{P}\cdot\boldsymbol{v})[\zeta_j + (1+p/r)\cos\theta_j] + (\boldsymbol{P}\cdot\boldsymbol{u})(p/r)\sin\theta_j\}$, $\theta_j = \theta - (j-1)\frac{\pi}{2}$, $j = 1, 2$, is clearly more demanding that the one of Equations (51) and (52), cf. [92]. The convenience of using C and S instead of ζ_1 and ζ_2 was realized by the developers of the Dromo software in [65], where they preferred to derive the hodographic velocities analytically as the arbitrary integration constants stemming from the solution of Equation (90) for the Keplerian case, in which $\boldsymbol{P}^*$ vanishes.

References

1. Encke, J.F. Über eine neue Methode der Berechnung der Planetenstörungen von J. F. Encke. *Astron. Nachrichten* **1852**, *33*, 377–398. [CrossRef]
2. Cowell, P.H.; Crommelin, A.C.D. The Orbit of Jupiter's Eighth Satellite. *Mon. Not. R. Astron. Soc.* **1908**, *68*, 576. [CrossRef]
3. Cowell, P.H.; Crommelin, A.C.D. Investigation of the Motion of Halley's Comet From 1759 to 1910. *Greenwich Obs. Astron. Magn. Meteorol. Made R. Obs. Ser. 2* **1910**, *71*, 1–84.
4. Battin, R.H. *An Introduction to the Mathematics and Methods of Astrodynamics*; American Institute of Aeronautics and Astronautics, Inc.: Reston, VA, USA, 1999.
5. Kustaanheimo, P.; Stiefel, E. Perturbation theory of Kepler motion based on spinor regularization. *J. Für Die Reine Und Angew. Math. (Crelles J.)* **1965**, *1965*, 204–219. [CrossRef]
6. Stiefel, E.L.; Scheifele, G. *Linear and Regular Celestial Mechanics*, 1st ed.; Grundlehren der Mathematischen Wissenschaften Series; Springer: Berlin/Heidelberg, Germany, 1971; Volume 174, pp. X, 306. ISBN 978-3-642-65029-1.
7. Ferrandiz, J.M. A new set of canonical variables for orbit calculations. In *ESA Proceedings of the Second International Symposium on Spacecraft Flight Dynamics*; SEE N87-25354 19-18; ESA Special Publication: Darmstadt, Germany, 1986; Volume 255, pp. 361–364.
8. Ferrándiz, J.M. A general canonical transformation increasing the number of variables with application to the two-body problem. *Celest. Mech.* **1988**, *41*, 343–357. [CrossRef]
9. Tisserand, F. *Traité de Mécanique Céleste. Tome I: Perturbations des Planètes d'aprés la Méthode de la Variation des Constantes Arbitraries*; Gauthier-Villars et fils: Paris, France, 1889.
10. Roy, A.E. *Orbital Motion*, 4th ed.; Institute of Physics Publishing: Bristol, UK, 2005; pp. XVIII+526.
11. Arsenault, J.L.; Ford, K.C.; Koskela, P.E. Orbit determination using analytic partial derivatives of perturbed motion. *AIAA J.* **1970**, *8*, 4–12. [CrossRef]
12. Broucke, R.A.; Cefola, P.J. On the Equinoctial Orbit Elements. *Celest. Mech.* **1972**, *5*, 303–310. [CrossRef]
13. Hintz, G. Survey of Orbit Element Sets. *J. Guid. Control Dyn.* **2008**, *31*, 785–790. [CrossRef]
14. Strömgren, B. Formeln zur genaeherten Stoerungsrechnung in Bahnelementen. Angewandt auf die Planeten 633 Zelima, 956 [1921 IW], 979 Ilsewa, 1035 Amata und 1049 [1925RB]. *Publ. Og Mindre Meddeler Fra Kobenhavns Obs.* **1929**, *65*, 1–26.
15. Milankovitch, M. *Kanon der Erdbestrahlung und seine Anwendung auf das Eiszeitenproblem*; Mechanics of Space Flight; Königlich Serbische Akademie: Belgrade, Serbia, 1941. English Translation: Canon of Insolation and the Ice-Age Problem. Israel Program for Scientific Translations, Jerusalem, 1969.
16. Herrick, S. Icarus and the variation of parameters. *Astron. J.* **1953**, *58*, 156–164. [CrossRef]
17. Musen, P. Special perturbations of the vectorial elements. *Astron. J.* **1954**, *59*, 262–267. [CrossRef]
18. Herget, P. On the variation of arbitrary vectorial constants. *Astron. J.* **1962**, *67*, 16. [CrossRef]
19. Allan, R.R. Satellite orbit perturbations due to radiation pressure and luni-solar forces. *Q. J. Mech. Appl. Math.* **1962**, *15*, 283–301. [CrossRef]
20. Allan, R.R.; Ward, G.N. Planetary equations in terms of vectorial elements. *Proc. Camb. Philos. Soc.* **1963**, *59*, 669. [CrossRef]
21. Roy, A.E.; Moran, P.E. Studies in the Application of Recurrence Relations to Special Perturbation Methods. III. Non-Singular Differential Equations for Special Perturbations. *Celest. Mech.* **1973**, *7*, 236–255. [CrossRef]
22. Deprit, A. Ideal elements for perturbed Keplerian motions. *J. Res. Natl. Bur. Stand.* **1975**, *79*, 1–15. [CrossRef]
23. Deprit, A. Dynamics of orbiting dust under radiation pressure. In *The Big-Bang and Georges Lemaître*; Berger, A., Ed.; Springer: Dordrecht, The Netherlands, 1984; pp. 151–180. [CrossRef]
24. Breiter, S.; Ratajczak, R. Vectorial elements for the Galactic disc tide effects in cometary motion. *Mon. Not. R. Astron. Soc.* **2005**, *364*, 1222–1228. [CrossRef]

25. Correia, A.C.M.; Laskar, J.; Farago, F.; Boué, G. Tidal evolution of hierarchical and inclined systems. *Celest. Mech. Dyn. Astron.* **2011**, *111*, 105–130. [CrossRef]
26. Katz, B.; Dong, S.; Malhotra, R. Long-Term Cycling of Kozai-Lidov Cycles: Extreme Eccentricities and Inclinations Excited by a Distant Eccentric Perturber. *Phys. Rev. Lett.* **2011**, *107*, 181101. [CrossRef] [PubMed]
27. Rosengren, A.J.; Scheeres, D.J. On the Milankovitch orbital elements for perturbed Keplerian motion. *Celest. Mech. Dyn. Astron.* **2014**, *118*, 197–220. [CrossRef]
28. Lara, M.; Rosengren, A.J.; Fantino, E. Non-singular recursion formulas for third-body perturbations in mean vectorial elements. *Astron. Astrophys.* **2020**, *634*, 1–9. [CrossRef]
29. San-Juan, J.F.; López, R.; Lara, M. Vectorial formulation for the propagation of average dynamics under gravitational effects (IAC-23,C1,8,3,x78887). In Proceedings of the 74th International Astronautical Congress (IAC), Baku, Azerbaijan, 2–6 October 2023; pp. 1–10.
30. Fehlberg, E. *Classical Fifth-, Sixth-, Seventh- and Eighth-Order Runge-Kutta Formulas with Stepsize Control*; NASA Technical Report NASA TR R-287; Marshall Space Flight Center: Huntsville, AL, USA, 1968.
31. Shampine, L.F.; Gordon, M.K. *Computer Solution of Ordinary Differential Equations: The Initial Value Problem*; Freeman and Co.: San Francisco, CA, USA, 1975; p. 318.
32. Dormand, J.R.; Prince, P.J. A family of embedded Runge-Kutta formulae. *J. Comput. Appl. Math.* **1980**, *6*, 19–26. [CrossRef]
33. Hairer, E.; Nørset, S.P.; Wanner, G. *Solving Ordinary Differential Equations I. Non-Stiff Problems*, 2nd ed.; Springer: Berlin/Heidelberg, Germany, 2008.
34. Sperling, H. Computation of Keplerian Conic Sections. *ARS J.* **1961**, *31*, 660–661. [CrossRef]
35. Burdet, C.A. Theory of Kepler motion: The general perturbed two body problem. *Z. Angew. Math. Und Phys.* **1968**, *19*, 345–368. [CrossRef]
36. Nacozy, P. The Intermediate Anomaly. *Celest. Mech.* **1977**, *16*, 309–313. [CrossRef]
37. Kamel, A. New nonsingular forms of perturbed satellite equations of motion. *J. Guid. Control Dyn.* **1983**, *6*, 387–392. [CrossRef]
38. Szebehely, V.; Bond, V. Transformations of the Perturbed Two-Body Problem to Unperturbed Harmonic Oscillators. *Celest. Mech.* **1983**, *30*, 59–69. [CrossRef]
39. Sharaf, M.A.; Awad, M.E.S.; Najmuldeen, S.A.S.A. Motion of artificial satellites in the set of Eulerian redundant parameters (III). *Earth Moon Planets* **1992**, *56*, 141–164. [CrossRef]
40. Fukushima, T. New Two-Body Regularization. *Astron. J.* **2007**, *133*, 1–10. [CrossRef]
41. Ferrer, S.; Lara, M. Families of Canonical Transformations by Hamilton-Jacobi-Poincaré Equation. Application to Rotational and Orbital Motion. *J. Geom. Mech.* **2010**, *2*, 223–241. [CrossRef]
42. Roa, J. *Regularization in Orbital Mechanics: Theory and Practice*; De Gruyter Studies in Mathematical Physics Series; De Gruyter: Berlin, Germany; Boston, MA, USA, 2017; Volume 42. [CrossRef]
43. Stiefel, E. Remarks on Numerical Integration of Keplerian Orbits. *Celest. Mech.* **1970**, *2*, 274–281. [CrossRef]
44. Urrutxua, H.; Peláez, J.; Bombardelli, C. Impact of the integration stop-condition on the accuracy of regularized orbit formulations (AAS 16-353). *Adv. Astronaut. Sci.* **2016**, *158*, 2503–2516.
45. Lara, M. Note on the analytical integration of circumterrestrial orbits. *Adv. Space Res.* **2022**, *69*, 4169–4178. [CrossRef]
46. Fukushima, T. Efficient Orbit Integration by Manifold Correction Methods. *Ann. N. Y. Acad. Sci.* **2005**, *1065*, 37–43. [CrossRef] [PubMed]
47. Hairer, E.; Lubich, C.; Wanner, G. *Geometric Numerical Integration. Structure-Preserving Algorithms for Ordinary Differential Equations*, 2nd ed.; Springer Series in Computational Mathematics; Springer: Berlin/Heidelberg, Germany, 2006; Volume 31, pp. XVI, 644. [CrossRef]
48. Fukushima, T. Further Simplification of the Manifold Correction Method for Orbit Integration. *Astron. J.* **2004**, *128*, 1446–1454. [CrossRef]
49. Barrio, R.; Serrano, S. Performance of perturbation methods on orbit prediction. *Math. Comput. Model.* **2008**, *48*, 594–600. [CrossRef]
50. Shefer, V.A. Application of KS-transformation in the problem of investigation of the motion of unusual minor planets and comets. *Celest. Mech.* **1990**, *49*, 197–207. [CrossRef]
51. Ferrandiz, J.M.; Sansaturio, M.E.; Pojman, J.R. Increased Accuracy of Computations in the Main Satellite Problem through Linearization Methods. *Celest. Mech. Dyn. Astron.* **1992**, *53*, 347–363. [CrossRef]
52. Martín, P.; Ferrándiz, J.M. Behaviour of the SMF Method for the Numerical Integration of Satellite Orbits. *Celest. Mech. Dyn. Astron.* **1995**, *63*, 29–40. [CrossRef]
53. Hansen, P.A. Auseinandersetzung einer zweckmässigen Methode zur Berechnung der absoluten Störungen der kleinen Planeten. Erste Abhandlung. *Abh. Der K. Sachs. Ges. Der Wiss.* **1857**, *5*, 41–218.
54. Musen, P. Application of Hansen's theory to the motion of an artificial satellite in the gravitational field of the Earth. *J. Geophys. Res.* **1959**, *64*, 2271–2279. [CrossRef]
55. Broucke, R.; Lass, H.; Ananda, M. Redundant Variables in Celestial Mechanics. *Astron. Astrophys.* **1971**, *13*, 390–398.
56. Deprit, A. Ideal Frames for Perturbed Keplerian Motions. *Celest. Mech.* **1976**, *13*, 253–263. [CrossRef]
57. Roa, J.; Kasdin, N.J. Alternative Set of Nonsingular Quaternionic Orbital Elements. *J. Guid. Control Dyn.* **2017**, *40*, 2737–2751. [CrossRef]

58. Breiter, S.; Langner, K. The Lissajous-Kustaanheimo-Stiefel transformation. *Celest. Mech. Dyn. Astron.* **2019**, *131*, 9. [CrossRef]
59. Amato, D.; Bombardelli, C.; Baù, G.; Morand, V.; Rosengren, A.J. Non-averaged regularized formulations as an alternative to semi-analytical orbit propagation methods. *Celest. Mech. Dyn. Astron.* **2019**, *131*, 21. [CrossRef]
60. Pirovano, L. Cataloguing Space Debris: Methods for Optical Data Association. Ph.D. Thesis, Surrey Space Centre, Department of Electrical and Electronic Engineering, Faculty of Engineering and Physical Sciences, University of Surrey, Guildford, UK, 2020.
61. Shuster, M. A Survey of Attitude Representations. *J. Astronaut. Sci.* **1993**, *41*, 439–517.
62. Abad, A.; Palacios, M.; Sein-Echaluce, M. An efficient formulation for numerical orbit computation. In *ESA, Spacecraft Flight Dynamics*; Hunt, J.J., Ed.; ESA Special Publication: Darmstadt, Germany, 1991; Volume 326, pp. 65–70.
63. Palacios, M.; Calvo, C. Ideal frames and regularization in numerical orbit computation. *J. Astronaut. Sci.* **1996**, *44*, 63–77.
64. Calvo, C. Integración Numérica de Problemas Orbitales en Sistemas de Referencia Ideales. Aplicaciones a Satélites Artificiales. Ph.D. Thesis, Universidad de Zaragoza, Zaragoza, Spain, 2000.
65. Baù, G.; Bombardelli, C.; Peláez, J. A new set of integrals of motion to propagate the perturbed two-body problem. *Celest. Mech. Dyn. Astron.* **2013**, *116*, 53–78. [CrossRef]
66. Urrutxua, H.; Sanjurjo-Rivo, M.; Peláez, J. DROMO propagator revisited. *Celest. Mech. Dyn. Astron.* **2016**, *124*, 1–31. [CrossRef]
67. Sundman, K.F. Mémoire sur le problème des trois corps. *Acta Math.* **1913**, *36*, 105–179. [CrossRef]
68. Szebehely, V. *Theory of Orbits. The Restricted Problem of Three Bodies*; Academic Press Inc.: New York, NY, USA; London, UK, 1967; pp. 1–668. [CrossRef]
69. Levi-Civita, T. Sur la résolution qualitative du problème restreint des trois corps. *Acta Math.* **1906**, *30*, 305–327. [CrossRef]
70. Bohlin, K. Note sur le problème des deux corps et sur une intégration nouvelle dans le problème des trois corps. *Bull. Astron. Ser. I* **1911**, *28*, 113–119. [CrossRef]
71. Brown, E.W.; Shook, C.A. *Planetary Theory*; Cambridge University Press: Cambridge, UK, 1933.
72. Deprit, A.; Elipe, A.; Ferrer, S. Linearization: Laplace vs. Stiefel. *Celest. Mech. Dyn. Astron.* **1994**, *58*, 151–201. [CrossRef]
73. Velez, C.E. Notions of Analytic Vs Numerical Stability as Applied to the Numerical Calculation of Orbits. *Celest. Mech.* **1974**, *10*, 405–422. [CrossRef]
74. Tapley, B.D.; Szebehely, V.G. The Regularization of Optimal Trajectories. *JPL Space Programs Summ.* **1967**, *4*, 5–9. Available online: https://ntrs.nasa.gov/api/citations/19670030904/downloads/19670030904.pdf (accessed on 24 September 2023).
75. Tapley, B.D.; Szebehely, V.; Lewallen, J.M. Trajectory optimization using regularized variables. *AIAA J.* **1969**, *7*, 1010–1017. [CrossRef]
76. McGehee, R. Triple collision in the collinear three-body problem. *Invent. Math.* **1974**, *27*, 191–227. [CrossRef]
77. Scheifele, G. On Nonclassical Canonical Systems. *Celest. Mech.* **1970**, *2*, 296–310. [CrossRef]
78. Ferrandiz, J.M.; Ferrer, S. A New Integrated, General Time Transformation in the Kepler Problem. *Bull. Astron. Inst. Czechoslov.* **1986**, *37*, 226.
79. Ferrándiz, J.M.; Ferrer, S.; Sein-Echaluce, M.L. Generalized Elliptic Anomalies. *Celest. Mech.* **1987**, *40*, 315–328. [CrossRef]
80. Scheifele, G.; Graf, O. Analytical satellite theories based on a new set of canonical elements. In Proceedings of the Mechanics and Control of Flight Conference, Anaheim, CA, USA, 5–9 August 1974; American Institute of Aeronautics and Astronautics: Reston, VA, USA, 1974; pp. 1–20. [CrossRef]
81. Cohen, C.J.; Hubbard, E.C. A nonsingular set of orbit elements. *Astron. J.* **1962**, *67*, 10–15. [CrossRef]
82. Lara, M. Note on the ideal frame formulation. *Celest. Mech. Dyn. Astron.* **2017**, *129*, 137–151. [CrossRef]
83. Urrutxua, H. High Fidelity Models for Near-Earth Object Dynamics. Ph.D. Thesis, Escuela Técnica Superior de Ingenieros Aeronáuticos, Plaza del Cardenal Cisneros, Madrid, Spain, 2015.
84. Nacozy, P.E. Time elements. In Proceedings of the Satellite Dynamics Symposium, Sao Paulo, Brazil, 19–21 June 1974; Giacaglia, G.E.O., Stickland, A.C., Eds.; Springer: Berlin/Heidelberg, Germany; New York, NY, USA, 1975; pp. 16–26. [CrossRef]
85. Nacozy, P.E. Time Elements in Keplerian Orbital Elements. *Celest. Mech.* **1981**, *23*, 173–198. [CrossRef]
86. Arakida, H.; Fukushima, T. Long-Term Integration Error of Kustaanheimo-Stiefel Regularized Orbital Motion. II. Method of Variation of Parameters. *Astron. J.* **2001**, *121*, 1764–1767. [CrossRef]
87. Scheifele, G. Généralisation des éléments de Delaunay en mécanique céleste. Application au mouvement d'un satellite artificiel. *Acad. Des Sci. Paris C. R. Ser. B Sci. Phys.* **1970**, *271*, 729–732.
88. Samway, R.C. A Special Perturbation Method Based on Canonical Delaunay-Similar Elements with the True Anomaly as the Independent Variable. Ph.D. Thesis, Department of Aerospace Engineering and Engineering Mechanics, The University of Texas at Austin, Austin, TX, USA, 1973.
89. Scheifele, G. An analytical singularity-free orbit predictor for near-earth satellites. In Proceedings of the International Symposium on Spacecraft Flight Dynamics, Darmstadt, Germany, 18–22 May 1981; ESA Special Publication: Darmstadt, Germany, 1981; Volume 160, pp. 299–305.
90. Baù, G.; Bombardelli, C. Time Elements for Enhanced Performance of the Dromo Orbit Propagator. *Astron. J.* **2014**, *148*, 43. [CrossRef]
91. Vitins, M. Keplerian Motion and Gyration. *Celest. Mech.* **1978**, *17*, 173–192. [CrossRef]
92. Deprit, A. The elimination of the parallax in satellite theory. *Celest. Mech.* **1981**, *24*, 111–153. [CrossRef]
93. Floría, L. Canonical elements and Keplerian-like solutions for intermediary orbits of satellites of an oblate planet. *Celest. Mech. Dyn. Astron.* **1993**, *57*, 203–223. [CrossRef]

94. Lara, M. Analytical and Semianalytical Propagation of Space Orbits: The Role of Polar-Nodal Variables. In *Astrodynamics Network AstroNet-II. Astrophysics and Space Science Proceedings*; Gómez, G., Masdemont, J.J., Eds.; Springer: Cham, Switzerland, 2016; Volume 44, pp. 151–166. [CrossRef]
95. Cayley, A. On Hansen's lunar theory. In *Collected Mathematical Works*; Cambridge University Press: London, UK, 1890; Volume III, pp. 13–24.
96. Brown, E.W. *An Introductory Treatise on the Lunar Theory*; The University Press: Cambridge, UK, 1896.
97. Milnor, J. On the Geometry of the Kepler Problem. *Am. Math. Mon.* **1983**, *90*, 353–365. [CrossRef]
98. Eades, J.B., Jr. *Orbit Information Derived from Its Hodograph*; Technical Memorandum NASA-TM-X-63301; Goddard Space Flight Center: Greenbelt, MD, USA, 1968.
99. Altman, S.P. A Unified State Model of Orbital Trajectory and Attitude Dynamics. *Celest. Mech.* **1972**, *6*, 425–446. [CrossRef]
100. Chodas, P. *Application of the Extended Kalman Filter to Several Formulations of Orbit Determination*; Technical Note 224; University of Toronto Institute for Aerospace Studies: Toronto, ON, Canada, 1981.
101. Vittaldev, V.; Mooij, E.; Naeije, M.C. Unified State Model theory and application in Astrodynamics. *Celest. Mech. Dyn. Astron.* **2012**, *112*, 253–282. [CrossRef]
102. Garofalo, A.M. New set of variables for astronomical problems. *Astron. J.* **1960**, *65*, 117–121. [CrossRef]
103. Alfriend, K.T.; Coffey, S.L. Elimination of the perigee in the satellite problem. *Celest. Mech.* **1984**, *32*, 163–172. [CrossRef]
104. Lara, M.; San-Juan, J.F.; López-Ochoa, L.M. Proper Averaging Via Parallax Elimination (AAS 13-722). *Adv. Astronaut. Sci.* **2014**, *150*, 315–331.
105. Leimanis, E. *The General Problem of the Motion of Coupled Rigid Bodies about a Fixed Point*; Springer Tracts in Natural Philosophy; Springer: Berlin/Heidelberg, Germany, 1965.
106. Leubner, C. Correcting a widespread error concerning the angular velocity of a rotating rigid body. *Am. J. Phys.* **1981**, *49*, 232–234. [CrossRef]
107. Peláez, J.; Hedo, J.M.; Rodríguez de Andrés, P. A special perturbation method in orbital dynamics. *Celest. Mech. Dyn. Astron.* **2007**, *97*, 131–150. [CrossRef]
108. Deprit, A.; Rom, A. The Main Problem of Artificial Satellite Theory for Small and Moderate Eccentricities. *Celest. Mech.* **1970**, *2*, 166–206. [CrossRef]
109. Sharaf, M.A.; Awad, M.E.S.; Najmuldeen, S.A.S.A. The Motion of Artificial Satellites in the Set of Eulerian Redundant Parameters. *Earth Moon Planets* **1991**, *55*, 21–44. [CrossRef]
110. Bar-Itzhack, I.Y. New Method for Extracting the Quaternion from a Rotation Matrix. *J. Guid. Control Dyn.* **2000**, *23*, 1085–1087. [CrossRef]
111. Danby, J.M.A. *Fundamentals of Celestial Mechanics*, 2nd ed.; Willmann-Bell: Richmond, VA, USA, 1992.
112. Baumgarte, J. A New Time Element for A General Time Transformation. *Celest. Mech.* **1976**, *14*, 121–127. [CrossRef]
113. Baù, G.; Bombardelli, C.; Peláez, J.; Lorenzini, E. Non-singular orbital elements for special perturbations in the two-body problem. *Mon. Not. R. Astron. Soc.* **2015**, *454*, 2890–2908. [CrossRef]
114. Lara, M. *Hamiltonian Perturbation Solutions for Spacecraft Orbit Prediction. The Method of Lie Transforms*, 1st ed.; De Gruyter Studies in Mathematical Physics; De Gruyter: Berlin, Germany; Boston, MA, USA, 2021; Volume 54, pp. XV, 377. [CrossRef]
115. Alfriend, K.T.; Dasenbrock, R.; Pickard, H.; Deprit, A. The extended phase space formulation of the Vinti problem. *Celest. Mech.* **1977**, *16*, 441–458. [CrossRef]
116. Kaptanoğlu, S. Weakly canonical transformations and the path integral quantization. *Phys. Lett. B* **1981**, *98*, 77–82. [CrossRef]
117. Goldstein, H.; Poole, C.P.; Safko, J.L. *Classical Mechanics*, 3rd ed.; Addison-Wesley: New York, NY, USA, 2001.
118. Nacozy, P.; Scheifele, G. *Investigation of Highly Efficient Satellite Solution Methods*; Technical Report NASA-CR-138593; Goddard Space Flight Center: Greenbelt, MD, USA, 1974.
119. Bond, V.R.; Janin, G. Canonical Orbital Elements in Terms of an Arbitrary Independent Variable. *Celest. Mech.* **1981**, *23*, 159–172. [CrossRef]
120. Floria, L.; Caballero, R. A universal approach to the intermediate anomaly of Keplerian motion. *J. Phys. A Math. Gen.* **1995**, *28*, 6395–6404. [CrossRef]
121. Andoyer, H. Sur l'anomalie excentrique et l'anomalie vraie comme éléments canoniques du mouvement eliptique, d'après MM. T. Levi-Civita et G.-W. Hill. *Bull. Astron. Ser. I* **1913**, *30*, 425–429. [CrossRef]
122. Deprit, A. A Note Concerning the TR-Transformation. *Celest. Mech.* **1981**, *23*, 299–305. [CrossRef]
123. Bond, V.; Broucke, R. Analytical Satellite Theory in Extended Phase Space. *Celest. Mech.* **1980**, *21*, 357–360. [CrossRef]
124. Hill, G.W. Motion of a system of material points under the action of gravitation. *Astron. J.* **1913**, *27*, 171–182. [CrossRef]
125. Flury, W.; Janin, G. Accurate Integration of Geostationary Orbits with Burdet's Focal Elements. *Astrophys. Space Sci.* **1975**, *36*, 495–503. [CrossRef]